# Microbial Fuel Cell for Waste Water Treatment


## Author: Fabio Cameli

## Supervisor: Rakel Wreland Lindström


Degree project in Chemical Engineering
Second cycle



KTH Royal Institute of Technology
School of Chemical Science and Engineering
Stockholm, Sweden

23 February 2016

# Microbial Fuel Cell for Waste Water Treatment

**Fabio Cameli**

## Abstract

Microbial Fuel Cell is a novel technology that can be used for a waste water treatment in order to simultaneously remove carbonaceous matter and nitrogen while producing electrical power. Even if it is not an established technology so far, MFC could be a cost effective option for waste water treatment and the major challenge of this process will be the device scale-up. Exoelectrogenic bacteria are capable of converting the chemical energy of organic matter into electrical energy by transferring the electrons produced in the oxidation to the anode electrode.

This project focused on developing a single device for nitrification, denitrification and carbon removal. Two double air-cathode single chamber MFCs are used to test the feasibility of this process that could replace the biological unit in a waste water treatment train.

The cells tested in this study were manufactured with the purpose of achieving a high surface area on both the anode electrode (Vitreous carbon foam) and the air-cathode electrodes (metallic mesh with diffusion layer and active layer) with different catalysts for the reduction reaction (cobalt and platinum). The bacterial biofilm growth is a fundamental step and the cells Open Circuit Potential was monitored during all the start-up period to determine the microorganism acclimation: a three days lag period was observed in both cells before the potential rise. The second cell was forced to reach higher voltage through an anode polarization and that seems to positively affect the biofilm stability at lower voltages transferring a greater amount of electrons and hence obtaining a higher current and power generation. For this reason after three weeks of inoculation the second cell reached an open circuit potential of 0.76 V which is a promising value for such a system.

Electrochemical and biological tests were conduced in order to test the power production of the cell and the substrate removal from the waste water. Polarization curves were used to evaluate power generation (and the maximum production under a specific external load) and the cell voltage trend which is characterized by activation and ohmic losses: 32 $\mathrm{mW}/m^2$ and 41 $\mathrm{mW}/m^2$ are the power density normalized by cathode surface (72 $cm^2$) reached by respectively first and second cell. The experimental conditions were varied from low to high temperature and from low to high inlet flow rate but the most affecting phenomenon seems to be the biofilm formation since significant voltage drops were noticed after long closed circuit operation. Higher cell voltage characterized the second cell thanks to more active cathode (platinum catalyst used) and more negative bacterial biofilm but a bigger drop in current generation over time affects the system performance and the most reliable reason is the shorter acclimation time compared to the first cell.

Cyclic voltammetry tests were carried out on both electrodes to study the potential range of activity and determine an optimal operational voltage despite of mass transport or kinetic limitations.

Substrate removal tests at different retention times in power generation conditions (external load 100 $\Omega$) showed a relatively high total nitrogen consumption (maximum 72.2 %) for the first cell while lower values were achieved by the second system meaning that a longer acclimation period is beneficial for nitrifying and denitrifying bacteria to thrive on the cathode biofilm.

Effluent pH level are almost similar to the initial values probably because of nitrification and denitrification protons offset.

# Dedication

To all smiles given to me.

# Acknowledgement

This thesis would not have been possible without my supervisor Rakel Wreland Lindström who accepted me for this project and inspired my work with precious advices.
For constant technical and moral support I owe my deepest gratitude to Maria Varini.

It is a pleasure to thank those who made this thesis possible with their help:
Bo Karlsson for his high skills in cell construction;
Yohannes Kiros and Alagar Raj Paulraj for providing electrodes and assisting me in making new ones;
Javier Barrientos for BET analysis;
Hyeyun Kim for SEM images;
Andrzej Nowak for potentiostat teaching;
Erik K. Levlin for supplying waste water and Mila Harding for the biological analysis;
and all the pH students from the Applied Electrochemistry department who tried to help me and solve every problem I met.

A special citation goes to the "master" Renato Ferretti for his teachings that guided me in the last years and especially in this period.

# Contents

# List of Figures

# List of Tables

# Chapter 1

# Introduction

## 1.1 Background

Microbial fuel cells are an innovative technology that has gained remarkable attention by researchers as it recovers energy from low cost waste. The fundamental process of this bio-electrochemical system (BES) is the transformation of chemical energy into electrical energy operated by exoelectrogenic bacteria capable of producing electrons during the consumption of an organic or inorganic substrate. BES technologies are suitable for a wide range of application like: energy recovery from wastewater, bioremediation, desalination, metal recovery, production of reduced products as carbon compounds, hydrogen and methane [12].
This bacterial property can accomplish nutrient removal in a waste water treatment and this is the reason why waste water treatment plants showed interest in using this kind of devices as a cost saving step of the entire process train.
Bacteria in a sludge are self-replicating and they differ in the temperature ranges of stability but the most common microorganisms in microbial fuel cells are *Geobacter* and *Shewanella*. These exoelectrogens bacteria are still examined to exactly understand the mechanism of electron delivery from cell to extracellular compounds: they can transfer electrons thanks to self-produced mediators or nanowires. They are able to adhere on the anode electrode and colonize it producing a biofilm in three main steps: they first attach on the surface then start to create a one-layered biofilm and afterwards the cells in the biofilm mature until it reaches a complicated three-dimensional structure. These bacteria are also involved in metal reduction application since they can accomplish metal reduction through their metabolism so they show good skills for a waste water treatment process.
Shewanella oneidensis (Fig.1.1a) is a rod shaped gram-negative anaerobic proteobacteria whose dimensions vary from 2-3 $\mu m$ in length and 0.4-0.7 $\mu m$ in diameter. Geobacter sulfurreducens (Fig.1.1b) is also a rod shaped gram-negative anaerobic bacteria which shows both flagella and phili. Its dimensions are typically under 4 $\mu m$.
Organic matter present in a waste water is mainly composed by volatile acids, polysaccharides, proteins and alcohols.
It is possible to refer to organic and inorganic matter in terms of BOD and COD: the Biochemical Oxygen Demand (BOD) is a 5 days degradation test that estimates the oxygen required by biological organisms for their life cycle, the Chemical Oxygen Demand (COD) measures the full oxidation of all organic matter whether it is biodegradable or not.
The electrons of the oxidation reaction produced by bacterial biofilm on the anodic electrode can flow through an external circuit towards the cathode where they take part at a reduction reaction (typically the oxygen reduction) with protons flowing through the membrane to the cathode, producing electrical energy.


**(a)** Shewanella oneidensis bacterium

**(b)** Geobacter sulfurreducens bacterium

**Figure 1.1:** Most common exoelectrogens bacteria in waste water

### 1.1.1 MFC electrochemistry

According to electrochemical principles the electrodes should be immersed in two different environments so a separation between an anoxic liquor where the bacteria produce electrons and the aerated solution where oxygen consumes electrons in its reduction is necessary. The separator could be a ionic membrane that works as a barrier to species like substrate and oxygen but allows the ions to flow into the chambers: in fact the higher is the current density in the external circuit the greater should be the protons flux in the solution.
The simplest MFC with two solution chambers, a membrane and air bubbled in the cathodic chamber is shown in Fig.1.2.
The common voltage achieved by a Microbial Fuel Cell is between 0.3 and 0.7 V [12].
Total cell potential corresponds to the difference between cathodic and anodic voltage and they are adjusted to neutral pH since the cellular environment of microorganisms is at $pH = 7$. Cell voltage, $E$ is a function of external resistance, $R_{\text{ext}}$, and the current, $I$. These variables are linked together by the Ohm law:

$$E = IR_{\text{ext}} \tag{1.1}$$

It is common to measure the voltage drop across the external circuit since in a MFC the current is small. The maximum voltage produced is theoretically the OCV, the Open Circuit Voltage (or Open Circuit Potential), which can be really achieved only when the circuit is disconnected: infinite resistance, no current. The electromotive force of the system, $E_{emf}$, produced by the coupled redox reactions, is strictly related to thermodynamic relationships and can be calculated by Nernst equation:

$$E_{\text{emf}} = E^0 - \frac{RT}{nF} ln(\Pi) \tag{1.2}$$

where $E^0$ is the standard cell electromotive force, $R = 8.31447$ J/mol-K the universal gas constant, $T$ is the absolute temperature (K), $n$ is the number of electrons flowing through

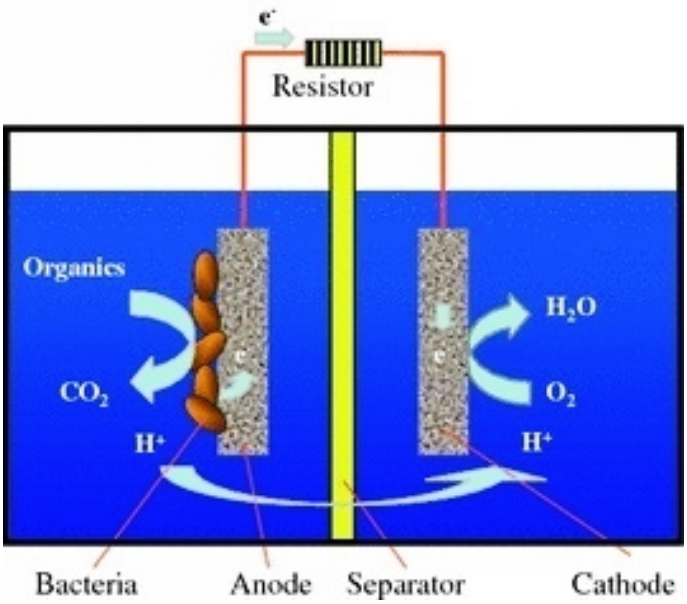


**Figure 1.2:** Basic microbial fuel cell

the circuit, and $F = 96485$ C/mol is Faraday constant. In this equation $\Pi$ is the reaction quotient which represents the ratio of products activities divided by reactants raised to their respective stoichiometric coefficients:

$$\Pi = \frac{[products]^p}{[reactants]^r} \tag{1.3}$$

According to IUPAC rules, the products are the reduced species and the reactants the oxidised species since the reactions are written as chemical reductions reactions.
In equation (1.2) the variables are calculated in standard conditions: temperature is assumed as 298 K, chemical concentrations are 1 M for liquids and 1 bar for gases. Also the values of $E^0$ are referred to hydrogen evolution under standard conditions, in which case $E^0(H_2) = 0$ and it is defined "Standard Hydrogen Electrode" (SHE).
The electromotive force is the total cell potential of the cell and it represents the difference between the cathode and the anode potentials, in this case they are adjusted to neutral pH and standard conditions: the correction for $pH = 7$ is expressed by $'$.

$$E'_{\text{emf}} = E'_{\text{Cat}} - E'_{\text{An}} \tag{1.4}$$

The overall cell potential ($E^0$) is decreased by

- *Ohmic losses*, $IR_\Omega$;
- *Cathodic and anodic overpotentials*, $OP_{\text{An}}$, $OP_{\text{Cat}}$ due to:
  - activation;
  - bacterial metabolism;
  - mass transport;

$$E_{\text{emf}} = E^0 - (\Sigma OP_{\text{An}} + |\Sigma OP_{\text{Cat}}| + IR_\Omega) \tag{1.5}$$

Ohmic losses are mainly due to ionic and electronic conduction so it is better to pack the electrodes, to enhance the electrolyte conductivity and to use a membrane with low resistance.
The activation polarization occurs at low current density because bacteria cannot transfer

electrons to the anode as they lost energy (as heat) to start the redox reactions.
Bacterial metabolism depends on the environment in which the microorganisms live and on the medium used in the solution in which they find nutrients but it is an intrinsic drawback of using bacteria as they need energy produced in the substrate oxidation.
Mass transport limitation is important when there is a significant difference between surface and bulk concentration: both substrate flux towards anode and proton flux from the anode can be limiting and cause this overpotential.
To relate the electrode potential to electrical current it is common to use Butler-Volmer equation (1.6) in which both cathodic and anodic contributes affect one electrode potential:

$$j = j_0 \cdot \left\{ exp\left[\frac{\alpha_a F \eta}{RT}\right] - exp\left[\frac{\alpha_c F \eta}{RT}\right] \right\} \tag{1.6}$$

in which:

- $j$: electrode current density ($A/m^2$);
- $j_0$: exchange current density ($A/m^2$);
- $\alpha_a$: anodic charge transfer coefficient (dimensionless);
- $\alpha_c$: cathodic charge transfer coefficient (dimensionless);
- F: Faraday constant (96485.33289 C/mol);
- R: universal gas constant (8.3144598 J/K-mol);
- T: absolute temperature (K);
- $\eta$: activation overpotential ($\eta = E - E_{eq}$);

Two limiting cases permit to simplify the Butler-Volmer equation:

- very low overpotentials, $|\eta| < RT/(nF)$ (c:a 25/n mV):

$$j = j_0 \cdot \frac{nF}{RT}\eta \tag{1.7}$$

- high potentials, $|\eta| > RT/(nF)$ the equation becomes linear and it is called Tafel equation:

$$\eta = a + b \cdot log|j| \tag{1.8}$$

  in which b is the Tafel slope and it is positive for anodic reaction ($E \gg E_{eq}$) and it is negative for the cathodic one ($E \ll E_{eq}$)

The average power produced in a Microbial Fuel Cell is usually in the range 4-15 $W/m^3$ [12]. It is possible to calculate the generated power from the measured voltage of the cell, $E_{\mathrm{MFC}}$, and the circulating current, $I$ as

$$P = IE_{\mathrm{MFC}} \tag{1.9}$$

and using the Ohm law (equation 1.1) it could be easily calculated from voltage and external resistance:

$$P = \frac{E^2_{\mathrm{MFC}}}{R_{\mathrm{ext}}} \tag{1.10}$$

or avoiding to use the cell voltage:

$$P = I^2 R_{\mathrm{ext}} \tag{1.11}$$

To better understand the efficiency of a device and compare different configurations and conditions is common to refer the generated power to the electrodes surface area, arbitrary the anode or the cathode.
The last parameter useful to evaluate the performance is Coulombic Efficiency that represents the extraction of electrons from the biomass as current and it is defined as:

$$C_E = \frac{Coulombs \quad recovered}{Total \quad coulombs \quad in \quad substrate} \tag{1.12}$$

Since the total charge (as Coulombs transferred in the system) is obtained from the current (I) and time elapsed it is possible to calculate Coulombic efficiency as

$$C_E = \frac{M_s \quad \int_0^t I\, dt}{F \quad b_{es} \quad \nu_{An} \quad \Delta c} \tag{1.13}$$

where $\Delta c$ is the change in substrate concentration (generally expressed as COD concentration) over the time ($t$), $M_s$ is the molecular weight of the substrate, F is the Faraday constant, $\nu_{An}$ is the volume of liquid in the anode chamber and $b_{es}$ are the electrons involved in substrate removal.

## 1.2 Waste water treatment application

MFCs is regarded as a fascinating technology for waste water treatment since it could be cost effective for a water treatment plant. In fact, according to Logan [12], the major costs for a waste water treatment plant are due to:

- *water aeration* (50% of total cost);
- *sludge treatment*;
- *water pumping*;

A MFC process could be a cost saving alternative since it can use an air-cathode avoiding to bubble air into the sewage like in the traditional aerobic treatment of Activated Sludge in which the bath needs to be constantly aerated. The cathode is exposed to air in which oxygen takes part in reduction reaction with ions and electrons on the surface of the electrode thanks to a diffusion layer that let it flow in the gas phase since oxygen has a higher solubility in air (21 %) compared to water ($\sim$ 8 mg/L).

It also requires less sludge treatment since it is an anaerobic process that typically produces less solid than an aerated one. This is the case of anaerobic processes for biogas production and carbon removal in which a energy consumption is necessary because mesophilic temperatures are required, hence a Microbial Fuel Cell could be even more efficient since it does not need energy input into the system and the power produced is immediately available as electrical energy while biogas needs further steps in energy production.

Then MFC is a power producer that could balance water pumping electricity demand which is a big issue for a water plant as the flow has to be directed in several pools and the need of pumps is a primary feature of such a plant.

The waste water tested in the cell used in this study came from Hammarby Sjöstadsverk which is located on top of Henriksdals WWTP in Stockholm. Henriksdal wastewater treatment plant (WWTP) is one of the world's biggest underground WWTP (approximately 90 % of facilities are located underground) and it is situated between Stockholm and Nacka and

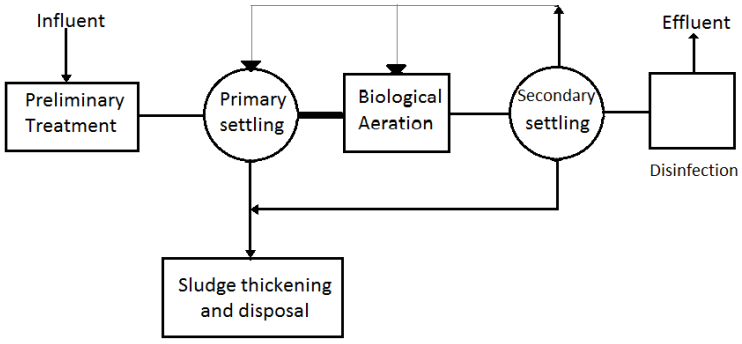


**Figure 1.3:** Common process flow train of a waste water treatment

it serves around one million people in Stockholm, Huddinge, Haninge, Nacka and Tyresö municipalities.
Managed by Stockholm water company (Stockholm Vatten) the plant occupies an area of 300000 $m^3$ with 18 Km of associated tunnels and a waste water treatment capacity of approximately 250000 $m^3/d$.
The processed water is emptied into the Baltic Sea after several different treatments as chemical, biological and mechanical processes.
An additional section for biogas production can provide the fuel for the heat production system that is converted into electricity available in the plant and it also distributes biomethane for vehicles. The final sludge deriving from the process is used as fertilizer.
The typical process flow train (Fig. 1.3) of a waste water treatment plant includes an aerated treatment (Activated Sludge) as biological step after preliminary screens (i.e. flow rate balance) and physical treatments as filtering and primary sedimentation then the secondary sedimentation provides the separation between the sludge (waste of the plant at the solid state after thickening) and the liquid coming from the aerated tank. The final process unit is usually a deeper removal of pollutant in the disinfection phase which can include chloride utilization.

## 1.3 Logan cell

Even if MFC are not an established technique there are some fixed points on which several researchers found their studies. Bruce E. Logan is by far the most active developer of Microbial Fuel Cell and his laboratory group in the Pennsylvania State University, Department of Civil and Environmental Engineering, is very productive in Microbial Electrochemical Technologies (METs) studies and publications.
Starting from the first basic cells they developed more efficient systems that allow them to focus on scale-up and economic issues besides substrate removal and power generation.
The latest cells produced in the Penn State University are all composed of two air-cathodes made of stainless steel meshes coated with a diffusion layer containing the catalyst (Activated Carbon) and graphite fiber brushes anodes. A textile separator seems to be the most efficient and cheap alternative to the previously used cation exchange membrane (often Nafion based). The last cell analysed by Logan's group (2015) [10] is showed in Fig.1.4 (front view and side sketch). In this cell the higher power production is achieved with the upstream flow (which assures a greater COD concentration) and higher power densities are due to bigger cathode area in which usually the limiting reaction takes place.

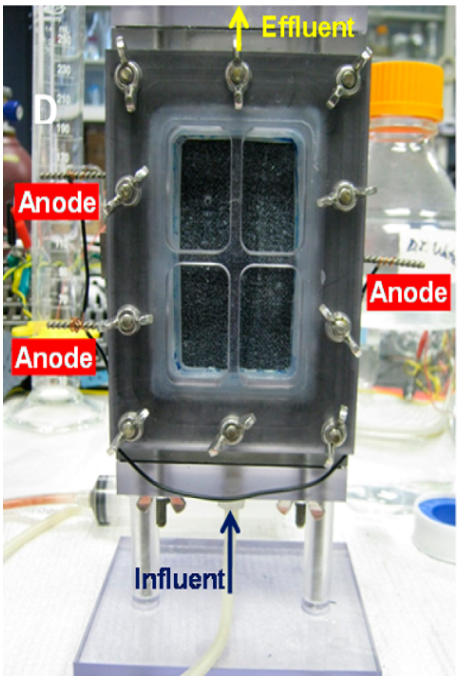


**(a)** Front view of Logan's last Microbial fuel cell

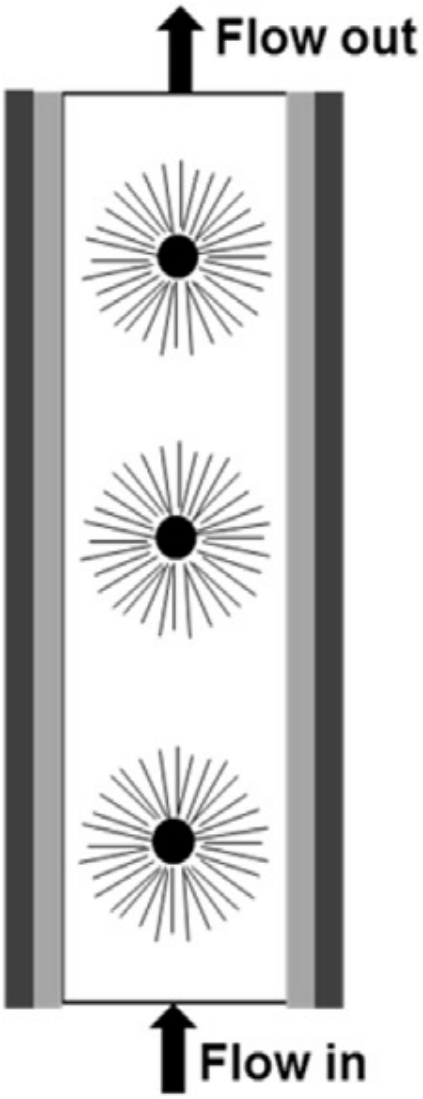


**(b)** Side view of Logan's last Microbial fuel cell

**Figure 1.4:** Last Microbial Fuel Cell developed by Logan's laboratory group

The Hydraulic Retention Time (HRT) is one of the most effective factor for cell performance: COD removal shows a proportional trend with HRT (a cell running with a 8.8h HRT reaches COD removal of $64.8 \pm 1.7$ %) and the CE is positively affected by an increase of HRT as well.
This kind of cell can go through a scale-up application and one of the most promising pilot plant designed is the 90-liter stackable microbial fuel cell showed in Fig.1.5 [2] that could operate in a self-sufficient mode for more than 6 months with an energy production of 0.097 $kWh/m^3$ used for the pumping system. Also the removal efficiencies are very high since for raw wastewater the COD removal was 87.6 %.

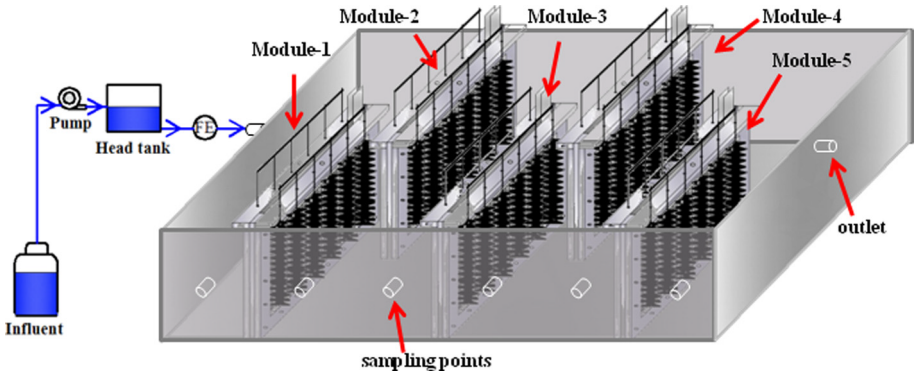


**Figure 1.5:** Pilot 90L stackable MFC

## 1.4 Scale-up

The main challenge of this technology as a waste water treatment application is the scale-up to industrial sizes [13]. As the industrial application is not established yet, the majority of researches has so far focused on laboratory scale in order to examine the different cell configurations and bacterial environments.
To reach a widespread usage in large scales these devices should overwhelm some problems mostly related to high costs of cell components. They can be enumerated as:

- *Membrane*;
- *Catalyst*;
- *Electrodes materials*;

According to latest studies it is possible to avoid the use of a membrane since a textile separator can be even more efficient and much cheaper than a cation membrane previously used: as the membrane, the separator can allow the ionic flux (protons) from the anode to the cathode and prevent the oxygen intrusion in the anoxic anodic chamber while protecting the system from short circuiting risk.

The choice of the catalyst is another big issue for total cost and overall efficiency: the mostly used platinum catalyst can be replaced by cheap materials with good catalytic properties as non-precious metal catalyst such as activated carbon that is the newest cathode catalyst in this field. The low price, the high activity and the wide range of sources (also renewable) make this material the most attractive catalyst for microbial fuel cell so far. However it is difficult to reach the same cell potential and performances over a long period of utilization of this catalyst are still unknown and not yet studied.

The electrode materials price is not a limiting question as it is commonly known that carbon based electrodes as graphite fiber for anode and common stainless steel mesh for cathode can achieve excellent results in substrate removal and power generation.
For these reasons the scale-up step should follow some main guidelines:

- use an air-cathode:
  an air-cathode is the best choice for the electrode as it allows to avoid the use of an air sparger that dramatically affects the total cost of the project;

- use cheap electrodes materials:
  the anode materials can be both efficient and cheap if they come from graphite or carbon such as carbon fiber brushes used in latest studies by several researches;

- use non-precious catalyst:
  a non-precious catalyst is perfectly suitable for an industrial application more than platinum and other noble metals used in former configurations, so activated carbon and non-noble metal based catalysts are the mostly studied materials for the scale-up.

- use closely spaced electrodes;
  the internal resistance in the solution is one of the limiting factor for power production so the best configuration for high dimensions requires closely spaced electrode. In this way the electrolyte resistance is decreased and it is easier to reach higher cell voltages;

- maximize electrode packing:
  in every industrial project the dimensions are very important in terms of materials cost and space occupied so in this application it is necessary to assure an optimal electrode packing and make the device as compact as possible.

## 1.5 Research scope

The main aim of this study is to test a microbial fuel cell with a municipal waste water coming from Henriksdal plant in Stockholm. The purpose is to use the MFC process instead of the biological unit of nitrification and denitrification and combining carbon removal at the same time.

### 1.5.1 Cell reactions

Since the device is a galvanic cell two electrochemical reactions take place at the cell electrodes.
On the cathode surface oxygen from the air gets reduced so the cathodic reaction is:

$$O_2 + 4H^+ + 4e^- \rightarrow 2H_2O \qquad E^{0'} = +0.805V \tag{1.14}$$

The anodic reaction involves organic compounds oxidation which provides electrons transferred to the electrode by the bacteria. Many carbonaceous substrates are present in a waste water and all of them take part in a oxidation reaction with different potentials.
Glucose was added in this study to provide more nutrient to microbial community, which produces electrons and carbon dioxide in anaerobic conditions (anodic bulk solution):

$$C_6H_{12}O_6 + 6H_2O \rightarrow 6CO_2 + 24H^+ + 24e^- \qquad E^{0'} = -0.428V \tag{1.15}$$

### 1.5.2 Nitrification-Denitrification

Biological nitrification is an oxidation reaction and it is carried out by aerobic bacteria which oxidise ammonia present in water as ammonium in nitrite and nitrate (eq. 1.16-1.17)[1].

$$NH_4^+ + 2H_2O \longrightarrow NO_2^- + 6e^- + 8H^+ \tag{1.16}$$

$$NO_2^- + H_2O \longrightarrow NO_3^- + 2e^- + 2H^+ \tag{1.17}$$

Bacteria need oxygen for the reaction and high pH consuming alkalinity.
Denitrification is a reduction reaction and it is realized by anaerobic bacteria that turn nitrate into nitrogen gas (eq. 1.18) and it is the most challenging process for the device since denitrifying bacteria need an electron donor that could be an organic compound, an inorganic matter or the cathodic electrode which receives electrons by the anode [1].

$$NO_3^- + 5e^- + 6H^+ \longrightarrow 1/2N_2 + 3H_2O \tag{1.18}$$

Nitrogen cycle of oxidation (Nitrification), reduction (Denitrification) and deammonification (Anammox) is shown in figure below. In common plants nitrification and denitrification

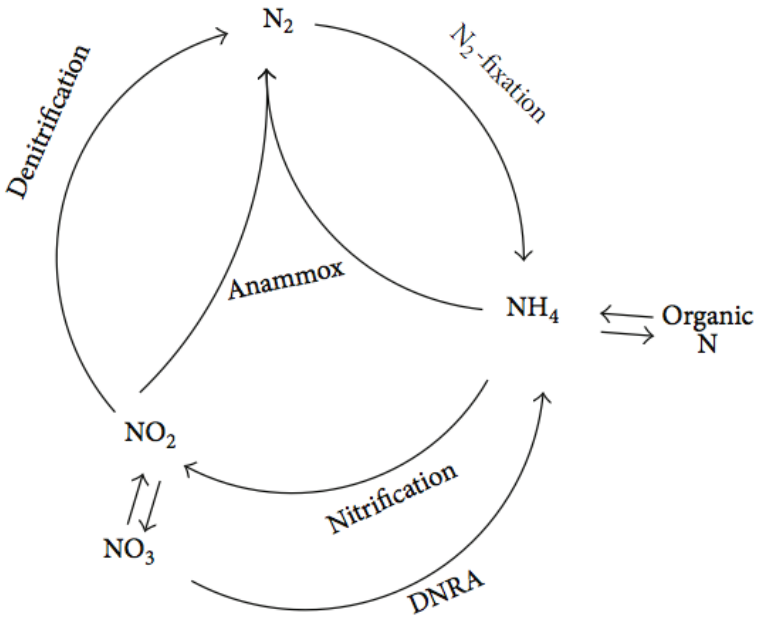


**Figure 1.6:** Nitrogen Cycle

take part in two different pools because they differ in oxygen demand and denitrification often need an electron donor addition that is expensive and sometimes toxic (i.e. methanol). In a microbial fuel cell nitrification and denitrification could be simultaneous since the air-cathode provides oxygen for ammonium oxidation while the anoxic chamber and electrons on the cathode enhance nitrate reduction into nitrogen by denitrifying bacteria [18, 19].
It could be possible to divide the processes into two devices for nitrification (aerated bath) and denitrification (MFC with nitrate removal).

### 1.5.3 COD removal

The Chemical Oxygen Demand removal is an important feature to express the performance of a MFC and a fundamental parameter to evaluate the feasibility of this technology for the waste water treatment. Both the rate and the percentage of removal are useful and different conditions of Hydraulic Retention Time and external load can affect the final COD

concentration that should be suitable for wastewater discharge.
Several phenomenons can cause changes in COD removal as microbial growth under current production conditions, aerobic reactions favoured by oxygen intrusion in the anodic chamber through the air-cathode and anaerobic bacteria development when another final electron acceptor is used in the waste water such as carbon dioxide.
A cell with a high surface area anode is most likely characterized by anaerobic processes while oxygen diffusion from the outside is responsible for aerobic COD removal. In any case the COD consumed by current production mechanisms cannot be separated from the other forms as anaerobic and aerobic processes [21].
The kind of wastewater used to feed the cell is also an important aspect in COD removal because a raw water (in this study the water was filter at 0.09 mm to avoid bacteria filtration) can produce additional substrate deriving from particulate COD, and it is also noticed that for a filtered water (0.4 $\mu m$) the COD removal can be fitted with a first-order reaction (eq. 1.19)but with two stages characterized by two different rates: one related to immediately ready COD and one due to slowly-degradable COD.

$$\ln(COD_t/COD_0) = -kt \tag{1.19}$$

In previous research different external loads (including Open Circuit Potential control) were applied in order to evaluate the higher COD removal rate which was recorded with a 100 $\Omega$ resistance that is also responsible for the higher power production in most cells [21].
The COD removal is also a function of the Hydraulic Retention Time and it has been proved that a higher HRT enhance the consumption. Also the system geometry can be mentioned as a influential factor in COD removal but it seems like it has more impact on power generation than Retention Time [10].

# Chapter 2

# Materials and methods

## 2.1 Cell set-up

Two different cells were developed in this work: they have the same geometry and components but they differ in cathodes materials. Each of them is composed of: a rectangular cell made by a Plexiglass chamber (6cm x 6cm x 2cm inner volume), two metallic mesh (nickel for the first one, stainless steel for the second one) based air-cathodes on the external faces and two sheets of activated carbon foam in the centre.
The components of the cells are represented in Fig. 2.1.

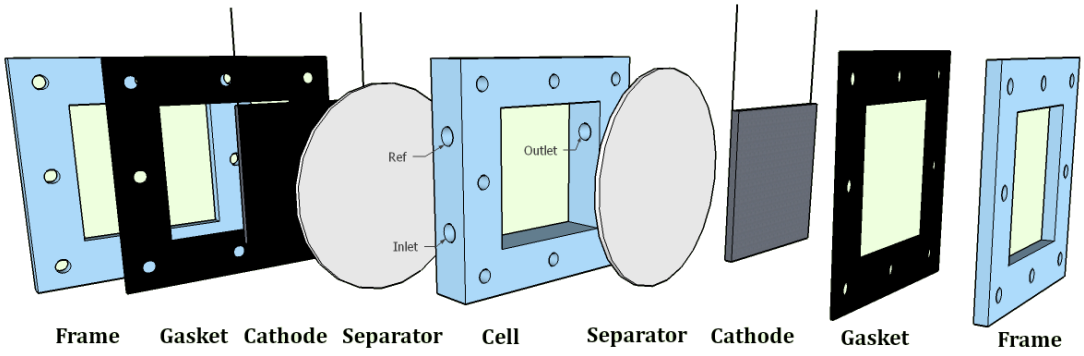


**Figure 2.1:** Cell set-up: Plexiglass chamber with holes for inlet and outlet solutions and for the reference electrode; Glass fiber separator; Metallic mesh based air-cathode; Rubber gasket; Frame. All components are symmetrical since two cathodes are placed in both sides of the cell.

### Single chamber

The Plexiglass structure contains the solution and the anode electrode. Three holes are drilled in the cell walls: one for the inlet water (downside), one (upside) for the reference electrode (Ag/AgCl electrode, immersed in KCl solution, which standard electrode potential $E^0$ against standard hydrogen electrode (SHE) is 0.197 V) and the last one is on top of the opposite wall for the effluent liquid from the cell. In this way the solution makes a upstream path that should lead to higher performances on substrate removal and power production [10]. Three autoclavable fittings (3 mm external diameter, Watson-Marlow) were screwed into the holes and connected to the pump tubes that provided the inlet flow to the cell and carried the effluent out of the device.

### Pump

A two channels peristaltic pump (Watson-Marlow 400FD/D2) was used in this work and it provided a constant flow rate through two tubes made of Bioprene (0.5 mm bore, 1.0 mm wall) connected through two autoclavable fittings (tube bore 3 mm) to autoclavable tubes (3 mm bore, 1 mm wall) transferring the solution from the flask to the cell.

### Anode electrode

The activated carbon foam (Vitreous carbon foam 3000C Goodfellow) is a good electrode [8] since it has an open pore structure and very high porosity so the surface is high as well and it shows low resistance to fluid flow. It is also chemically inert in non-oxidising environments over a wide temperature range, it maintains strength at high temperatures and it is thermally insulating and electrically conductive. Its applications include also thermal insulation, filtration, substrate support and acoustic control. The high porosity is the most attracting feature for using this material as the anode since it favours bacteria growth on its surface. The activation of the electrode has been accomplished with an acidic treatment with nitric acid and its procedure is explained in a following section .
The main features of the carbon foam are listed below:

- Bulk density: 0.05 $g/cm^3$;
- Porosity: 96.5 %;
- Pores/cm: 24

**Figure 2.2:** Anode electrode

The two papers of carbon foam (6cm x 6cm x 0.5cm) are tightened together by a titanium wire (99.7 % purity, diameter 0.25 mm, resistivity 42.0 $\mu\Omega - cm$, 20 °C Sigma-Aldrich) that works also as current collector for electrons flowing through the external circuit: this material is the best choice for its good resistance to corrosion and high biocompatibility

(Fig. 2.2). The titanium wire comes out from a hole on top of the cell in order to be available for the connection with the alligator of the Potentiostat (Reference 600 Potentiostat/Galvanostat/ZRA, Gamry Instruments) that collects the data of electrochemical measurements.

### Cathode electrode

Three different cathode electrodes were tested in the cells since the counter reaction (oxygen reduction) is often the limiting step of the process and the use of different catalysts was explored in order to reduce kinetic issues.

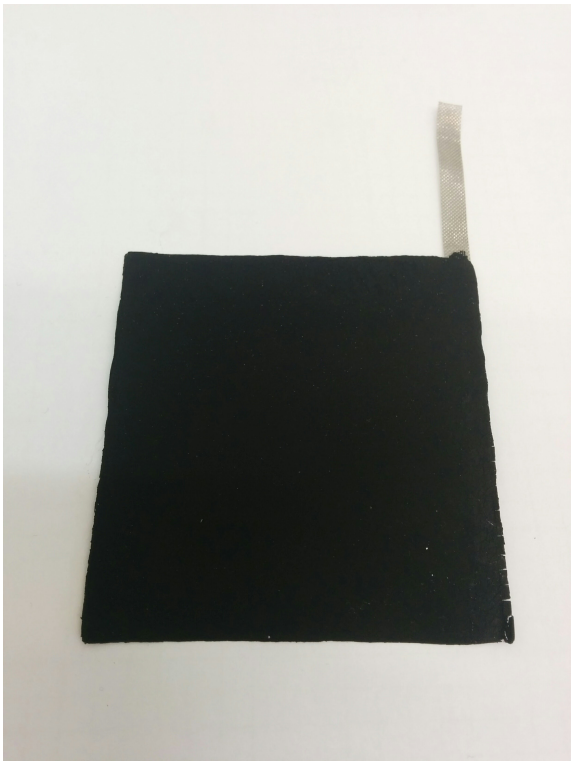

**Figure 2.3:** Cathode electrode used in the second cell

The cathodes used in the first cell have been realized with a small amount of cobalt as a catalyst and carbon black and PTFE (Polytetrafluoroethylene) as diffusion layer on a nickel mesh. Cobalt is as good catalyst with good performances as platinum widely used for this kind of device and it is cheaper compared to a noble metal catalyst. Cobalt tetramethoxyphenyl porphyrin mixed with carbon black (Ketjenblack EC-300N) was activated by a thermal treatment of pyrolysis.
The diffusion layer is very important for oxygen diffusion on the cathode surface and its hydrophobic characteristics due to PTFE avoid water leakage through the nickel mesh. This electrode was previously produced for oxygen reduction in alkaline environment and was used in this research to enhance the counter reaction on the cathode and make it non-limiting compared to the substrate oxidation on the anode which is supposed to be the principal reaction and the one that mainly affects the biofilm generation and power production. The same titanium wire used for the anode is pressed on the nickel mesh of each cathode to assure a good electric conduction between the electrode and the current collector and the two cathodes wires were twisted together so they acted as a single electrode for the alligator's clamp.
The second cell differed from the first one only for the cathodes electrodes which were realized exclusively for this cell: platinum was the catalyst chosen for the active layer and a

stainless steel mesh supported the active and diffusion layers produced for the experiment. The procedure followed to manufacture the cathodes is explained below in details.
The third cathode electrode produced was realized with the stainless steel mesh used in the second electrode and with a mixture of diffusion layer (PVDF based) and catalyst (activated carbon). This electrode was manufactured with the purpose of testing the cell with a cheap and scalable electrode but the recipe followed to make it was not suitable for big dimensions as the electrode utilized.
The procedures to manufacture the cathodes are reported in following section. The two different cathodes used in the cells look almost similar so only the second one (platinum catalyst) is shown in Fig. 2.3.

**Separator**

On each water side of the cathodes two glass fiber separators (Glass Microfibers Filters, borosilicate glass circles, diameter 90 mm, thickness 0.26 mm, pore size 1.6 $\mu m$, Whatman$^{TM}$ 1820-090) were used to reduce cathode biofouling and oxygen intrusion and to avoid a short-circuiting.
The water used in the study was not finely filtered so the cathode biofouling is supposed to be a big issue for the device and a protection for the electrode is strictly necessary.
The screen to oxygen diffusion is also very important for the anode chamber which is kept under anaerobic condition by the anoxic solution flowing inside and a oxygen intrusion in the cell can decrease the efficiency of the cell because aerobic bacteria can develop faster then the anaerobic ones that are the electrons suppliers to the anode electrode.
Even if the cells are single-chambered the separator is mandatory to prevent short-circuiting which can be favoured by the short distance between the two electrode that are closely spaced to make the cell as compact as possible.
The typical cation exchange membranes used before (like Nafion) can be replaced by such separator with an important decrease of cost and a high efficiency as it allows ions produced in the anodic chamber to flow towards the cathode electrode and this is fundamental for current generation since the higher the electrons flow through the external circuit the greater the ions flux into the solution to achieve a significant current produced. Other studies underlined the positive effects of glass fiber separators on the reduction of Microbial Fuel Cell start-up time as well [22].

**Gaskets**

Two rubber gaskets avoided water losses from the cell and they were tighten up with the cathodes by 8 stainless steel screws by two Plexiglass frames (with same cell dimensions to let the cathodes open to air and to block the separator, the cathode and the gasket against the main chamber's walls) that completed the cell set-up, showed in Figure below with a real image.

The experimental set up is shown in Fig.2.5: the cell is connected through a capillary to the reservoir in which the reference electrode is immersed and read the potential and that is hold by a metallic clamp above the cell.
The three holes flask in which the feeding solution is heated by the thermostat bath is connected to the inlet and outlet tubes and to the $N_2$ gas purging tube.
The three electrodes configuration of the potentiostat is guaranteed by the connection of the clamps of the instruments with the reference, the anode and the cathode electrodes.

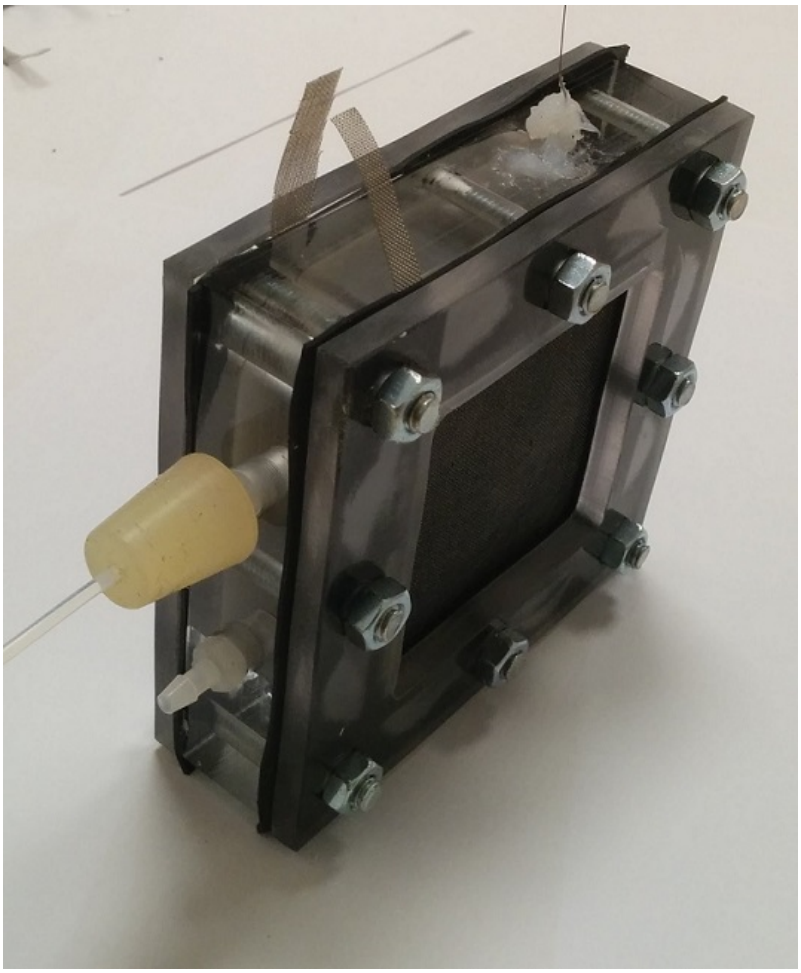

**Figure 2.4:** Real image of the cell

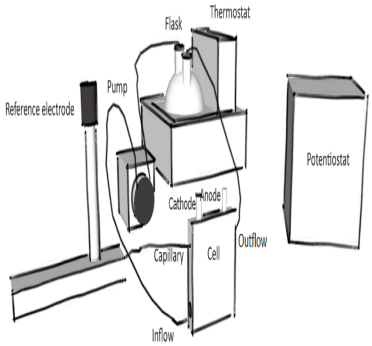


**(a)** Sketch of the experimental set-up.

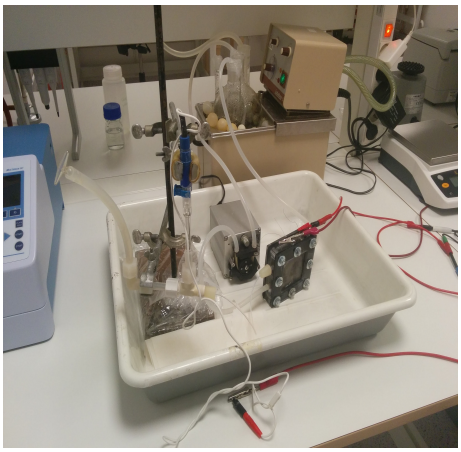

**(b)** Real image of experimental set-up.

**Figure 2.5:** Experimental set-up: the flask containing the feeding solution is heated by a thermostat bath and purged with $N_2$ while sending the inlet liquid through the pump to the cell which, as the reference electrode, is connected to the potentiostat.

### 2.1.1 Anode preparation

The vitreous carbon foam used for the anode electrode of both the two cells was activated with an acidic treatment according to previous scientific research [3]. A total volume of 600

mL of a 5% nitric acid solution was used for the process and the volumes calculation is shown in Appendix.
Before putting two foams (6cm x 6cm x 0.5cm each) into the liquid they have been poured into a 2-propanol solution [16] to fill the pores with the organic solvent and push the air outside, then the electrode has been immersed in water in order to clean it from the propanol and afterwards it was ready for the activation treatment.
A heater plate (*Framo−Gerätetechnik* M21/1) maintained at 125 °C guaranteed a thermal flux to the baker containing the solution with the foams, thereby the thermal treatment lasted 8 hours and after that the foams were washed for 15 min with a milli-Q water stream. The electrodes were hence ready to be dried in the oven (Heraeus D-6450 Hanau) at 110 °C for 14 hours.

To better understand the effects of the treatment on the foams some pictures were taken with the Scanning Electron Microscope and the different results obtained are compared in the next Chapter.

A further analysis was made on the foam to estimate its surface area and then refer the power produced to the anodic area. The Brunauer-Emmett-Teller (BET) measurement was affected by the porous structure of the foam that was not analysed in powder state but it was cut in small pieces and put into the glass tube of the instrument.
At the same time the instrument (ASAP 2000 micromeritics) can estimate the pore size distribution with the Barret-Joyner-Halenda (BJH) adsorption.
The nitrogen absorption necessary for the experiment was carried out in a bath at 77.35 K with a foam sample of 0.1154 g. The instrument recorded the nitrogen pressure (P, mmHg) in the tube containing the sample and the volume of nitrogen absorbed on the sample (Vad, $cm^3/g$ STP) while the saturation pressure of nitrogen (Ps) was 759.85132 mmHg.
The report of both experiments (BET and BJH analysis) is shown in the Appendix while the main results of the measurements are examined in the Result chapter.
All data obtained from the instrument were applied by the software to the BET linearized equation (2.1) that gives the graph represented in next chapter as the table containing the parameters of the equation: the BET surface area is the most interesting value since the surface determination was the main aim of the analysis.

$$\frac{1}{V_{ad}\left[(P_s/P)-1\right]} = \frac{1}{V_m C} + \frac{C-1}{V_m C}\left(\frac{P}{P_s}\right) \tag{2.1}$$

### 2.1.2 Cathode preparation

The cathodes used in the first cell were realized for Oxygen Reduction Reaction in previous research [11]. A nickel mesh was the support for the diffusion layer (Polytetrafluoroethylene based) and the catalyst layer obtained from cobalt tetramethoxyphenyl porphyrin mixed with carbon black (Ketjenblack EC-300N) using a thermal treatment of pyrolysis.

For the second cell two new cathodes were prepared in order to explore different performances of materials. According to the recipe elaborated in a recent paper [20] the cathodes were made of a stainless steel mesh covered with a mixture of activated carbon, carbon black and PVDF solution that accomplishes the catalyst and diffusion layer role at the same time.
Since Poly(vinylidene fluoride) (PVDF) is a hydrophobic polymer it is largely used as binder in diffusion layers for air-cathodes (PTFE is also utilized): the solution which contains this polymer was made of N,N-dimethylacetamide (DMAc) and PVDF powder (10 % w/v) and it was obtained by dissolving the powder into the solvent with magnetic stir overnight.
The stainless steel mesh is a good support as it is electrically conductive, porous and cheap

compared to other metals: it can work as a current collector for electrons flowing from the anode and can also let the ions reach the electrode surface to react with oxygen from the air.
In this study the grid was provided by Stockholms Plat & Gummiperforering SPG AB (mesh nr: 60, width: 1020 mm, weight: 0,71 $kg/m^2$) and its main features are listed below:

- Mesh: 0.25 mm;
- Wire: 0.15 mm;
- Material: AISI 316;
- Open area: 39 %;

For each cathode 1120 mg of AC powder (Norit KB-B Ba.♯ M-1223) and 112 mg of CB (Ketjenblack Akzo Chemie, The Netherlands) were mixed with 3.7 mL of PVDF solution prior to spread the mixture onto the 42,25 $cm^2$ stainless steel grid (6,5 x 6,5 cm) with a spatula and let the phase inversion trigger by putting the cathode into deionized (DI) water until the start of the building of the cell. Since the PVDF solution was very viscous and to use a pipette was little reliable because of formation of air bubbles, the solution was weighted and the exact amount is expressed in grams (3.162 g each cathode) and the calculations to obtain this value are reported in Appendix. The slurry spread onto the grid was very viscous and an homogeneous layer was hard to be achieved so after spreading it with a spatula the electrodes were calendered in order to achieve a fixed thickness and a smoother surface.
A first calender thickness of 1.7 mm was used to press the electrodes while the second and last step was to use a 1.2 mm thickness which is then the final thickness of the electrodes that were then immersed into deionized (DI) water. According to the original paper the electrode should be dried in a fume hood for more than 8 h and then stored in deionized (DI) water but in this case the electrodes were put into water overnight and taking them out of water only before using them in the cell so the drying step was postponed to prevent cracks on the surface.

The last cathodes were made at the same way of the ones used in the first cell: in that case a metal mesh (nickel) was used to support the diffusion layer (PTFE based) and the active layer (cobalt on Vulcan carbon). Similar electrodes were produced with the stainless steel mesh above mentioned and two layers pressed over it: a diffusion layer made by 80 % carbon black (Ketjenblack Akzo Chemie, The Netherlands) and 20 % of PTFE solution (60 %) in weight ratios and an active layer produced with the following weight proportions: 70 % Platinum on Vulcan carbon (20 % Pt on Vulcan XC-72 supplied by E-TEK) and 30 % PTFE solution (60 % Teflon in the solution).

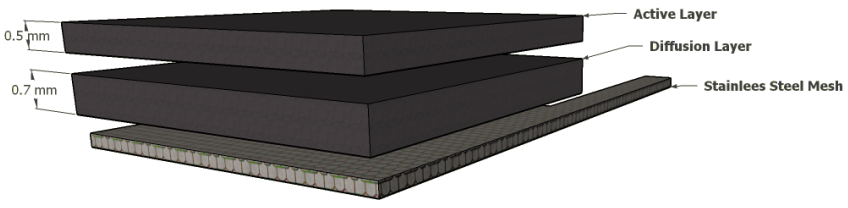


**Figure 2.6:** Sketch of the air-cathode used in the second cell

The active layer was produced by mixing the two reactants after adding drop-wise the Teflon solution in the carbon powder and then an hydrocarbon solvent (D-70) was added to bind the mixture and create a dough.
The next step was the roll of the mixture with a rolling press in which the thickness was decreased step-wise: 2.2 mm, 1.7 mm, 1.2 mm, 0.5 mm. At this point the diffusion layer was rolled as well at 0.7 mm and then rolled again on the stainless steel grid. Afterwards the active layer was rolled over the diffusion layer and the net (1.2 mm total thickness) and in order to press better the layers against the mesh the whole electrode was rolled at 1 mm.
The last step was the solvent removal and it was accomplished by pressing the electrodes (packed between two papers) with a press (Nike, Eskilstuna Sweden) at 355 $Kg/cm^2$ and then they were let dried in a calcination oven (Carbolite CWF 12/13, ab ninolab) up to 95 °C by increasing the temperature step-wise with a rate of 2 °C/min. In this way the solvent (D-70) was almost removed but since its evaporation temperature is 120 °C the complete evaporation of the solvent was accomplished by heating the samples in a $N_2$ atmosphere (Carbolite Eurotherm 2408) up to 330 °C so the solvent would be removed and also the emulsifier component in the PTFE solution could evaporate without damage the Teflon (that is stable until that temperature) and without risking to make the platinum particles burn since the $N_2$ avoids combustions.
In this case the active layer and the diffusion layer face the solution and a small plain piece of mesh is not covered with the layers in order to be used as current collector out of the cell and be connected with the external resistance. Figure 2.6 shows the schematic of the electrodes with the diffusion layer and the active layer rolled over the stainless steel mesh.

### 2.1.3 Reference electrode

The reference electrode of the cell is a commercial Ag/AgCl electrode (Radiometer Analytical XR300 14002-A02) immersed in a saturated solution of KCl and it needs to be in contact with the working solution so the connection was provided by a thin capillary put close to the anode surface (Fig.2.8) and that reaches through the upper port in the cell side the external structure where the reference sensor is located.
In Figure 2.7 it is shown the plastic equipment which collects the solution from the cell and supplies a hole to the reference sensor in which it can create a connection with the solution. At the end of this external structure a vertical plastic tube guarantees a water reservoir to balance the flow pressure of the solution on the reference.
The reference electrode sensor is connected with a wire which is coupled with the potentiostat alligator to collect data in a three electrodes configuration (with working and counter electrode completing the circuit).
The connection between the reference electrode and the inner cell environment provided by the capillary could affect the electrochemical measurements because of the ohmic loss due to the length of the capillary. Theoretically the reference electrode should be in touch with the same solution in which the working electrode is placed but the presence of solid deposits in the waste water solution that filled the capillary can have the same negative effect of bubbles on the reference potential record.
The influence of anomalous reference electrode behaviour is clear in the cyclic voltammetry measurements results shown in next chapter.
In the second cell another connection between the reference and the cell solution was provided: since the ohmic drop through the capillary is likely one of the most affective issues in the electrochemical tests, the interface between the reference and the inner solution was moved inside the cell and not at the end of the capillary as for the first cell. The same capillary used previously was in touch with the reference electrode in the external structure showed in Fig. 2.7 but it was filled with KCl (saturated, saturation 20 °C: 34 g/100g water) solution that is the same solution in which the reference electrode is

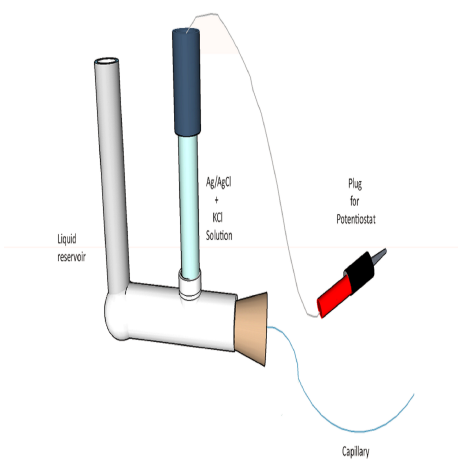


**(a)** Sketch of the reference electrode.

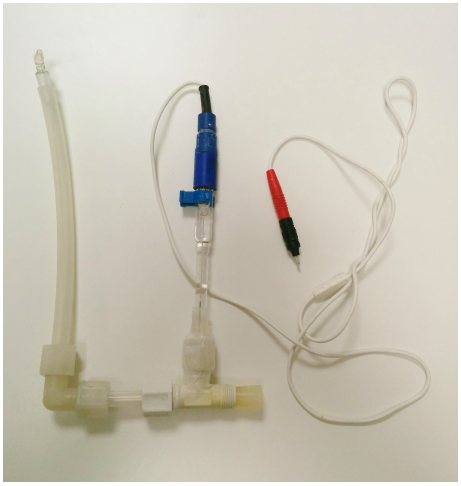

**(b)** Real image of reference electrode.

**Figure 2.7:** Reference electrode set-up: the reference sensor (contained in a Ag/AgCl + KCl solution) is immersed in the reservoir solution and connected to the cell with a capillary and to the potentiostat clamp with a metallic plug.

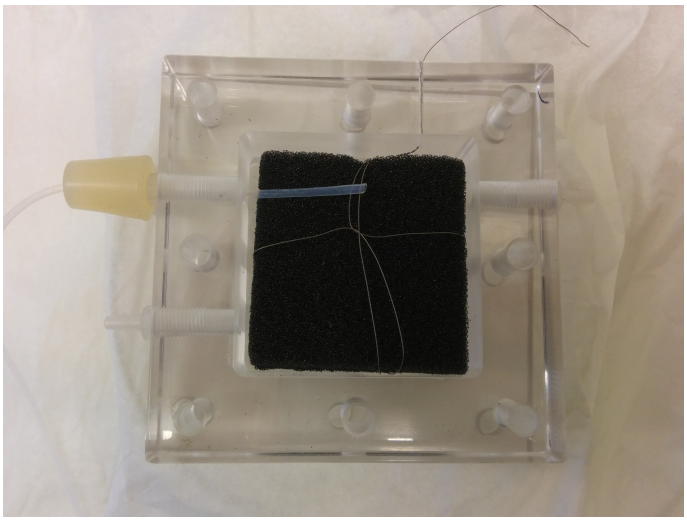

**Figure 2.8:** Internal capillary that connects the cell with the reference electrode

immersed and the opposite extremity was obstructed by a filter paper (Glass Microfibers Filters, borosilicate glass circles, diameter 90 mm, thickness 0.26 mm, pore size 1.6 $\mu m$, Whatman$^{TM}$ 1820-090) hence a physic separation was provided between the cell solution and the reference one and consistent ohmic losses were avoided.

## 2.2 Cell feeding solution

The electrolyte used in this project is composed by waste water (as bacteria source) and by a medium containing a PBS buffer solution and a mixture of minerals and vitamins that amends the water solution increasing the conductivity and stabilizing the pH.
Beside the substrate already present in the waste water a little amount of co-substrate (glucose 1 g/L) was added to enhance the bacteria growth and every supplement of fuel is reported in the experimental description.
The composition of inlet liquid is modified during the work to evaluate the magnitude of the contribute of different components (bacteria amount, conductivity, minerals and vitamins

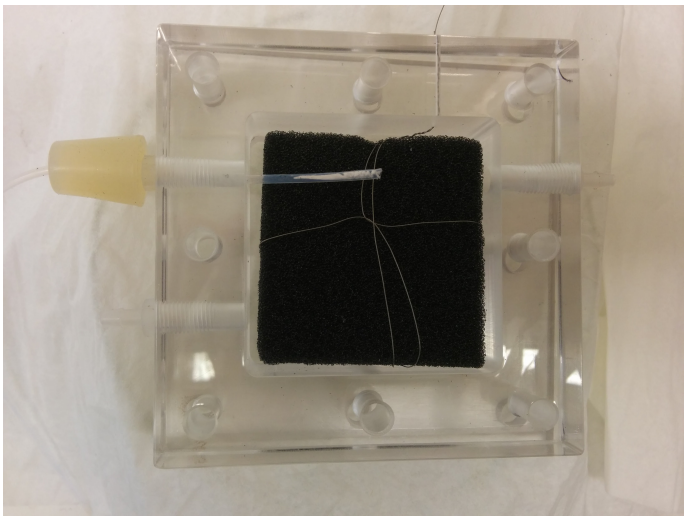

**Figure 2.9:** Internal capillary that connects the cell with the reference electrode filled with filter paper

nutrition) by comparing performance data at different conditions.

### 2.2.1 Waste water

The sewage feeding the cell derived from Stockholm City and it would have been sent to aerobic treatment after filtration and pre-sedimentation. Since the concentrations of substrate as nitrogen and COD were not monitored on-line it is useful to refer to average values during the day (the concentrations are very fluctuating).
It is common to refer to ammonium as nitrogen content (its around 60-70 % of total nitrogen amount) since nitrates ($NO_3$) and nitrites ($NO_2$) are often close to 0.
For these reasons the reference values of nitrogen and COD of the municipal wastewater sample are:

**Table 2.1:** Waste water features

| Feature | Value |
|---|---|
| Conductivity | 893 $\mu$ S/cm |
| Suspended solids SS | 163 mg/L |
| Alkalinity | 4,56 mmol/L |
| pH | 7.23 |
| COD | 334 mg/L |
| Phosphorus | |
| $PO_4 - P$ | 9.66 mg/L |
| Tot-P | 23.9 mg/L |
| Nitrogen | |
| $NH_4^+$ | 46.9 mg/L |
| $NO_3 - N$ | 0.33 mg/L |
| $NO_2 - N$ | 0.02 mg/L |
| Total-N | 54 mg/L |

Even if a genetic analysis has not been carried out, the waste water is used as bacteria source for the cell and it is supposed to contain a mixed culture of microorganism including the exoelectrogenic families cited above.

### 2.2.2 Cell medium

Beside the bacteria inoculation, the cell was fed with a medium that provided a buffer solution to control the pH level and stabilize it around neutral pH, a minerals and vitamins solution which could assure a good living environment for the microorganisms that found nutrients in the solution. In tables below are listed the components of these solutions and their concentrations.
The buffer solution was prepared following Logan's recipe using a 5 L solution that could provide a long time utilization. This phosphate buffer solution had a final molarity of 50 mM and its composition is showed in Table 2.2.

**Table 2.2:** Phospate Buffer Solution composition for 1L solution 50mM

| Ingredients | Mass(g) | Molecular weight (g/mol) | Concentration (mM) |
|---|---|---|---|
| $NH_4Cl$ | 0.31 | 53.5 | 5.79 |
| $NaH_2PO_4 \cdot H_2O$ | 2.452 | 137.99 | 17.77 |
| $Na_2HPO_4$ | 4.576 | 141.99 | 32.23 |
| $KCL$ | 0.13 | 74.5 | 1.74 |

The nutrient solution for bacteria was prepared from a vitamins mixture and the addition of several minerals. For 1 L solution were used:

**Table 2.3:** Vitamins composition for 1L solution

| Ingredients | Concentration (mg/L) |
|---|---|
| Beta-Carotene | 7 |
| vitamin A | 3.5 |
| vitamin D3 | 0.075 |
| vitamin E | 50 |
| vitamin C | 400 |
| vitamin B1 (thiamin) | 8 |
| vitamin B2 (riboflavin) | 10 |
| vitamin B3 (nicotinic acid) | 120 |
| vitamin B5 (pantothenic acid) | 25 |
| vitamin B6 (pyroxidine) | 9 |
| vitamin B7 (biotin) | 0.075 |
| vitamin B9 (folic acid) | 1.4 |
| vitamin B12 | 0.014 |

Both PBS solution and vitamins and minerals mixture were autoclaved in order to prevent contamination for bacteria culture using a Systec DX-23 autoclave at 121 °C for 20 min for the PBS and at 99 °C for 15 min for the vitamins and minerals (this temperature is conservative since it is an average value at which corresponds a low thermal degradation of vitamins that are more sensitive to heat than minerals as they are composed by cells and proteins). They were then stored in a fridge at 4 °C so they were ready for use.

## 2.3 Inoculation and biofilm growth

The two cells produced in this work were tested with Henriksdal plant filtered water (0.09 mm sieve diameter) amended with a medium solution made of PBS solution and vitamins and minerals with the following proportions:

**Table 2.4:** Minerals composition for 1L solution

| Ingredients | Concentration (g/L) |
|---|---|
| $Ca$ | 2.4 |
| $Mg$ | 0.56 |
| $MgSO_4 \cdot 7H_2O$ | 5.575 |
| $Fe$ | 0.08 |
| $FeSO_4 \cdot 7H_2O$ | 0.1 |
| $Zn$ | 0.06 |
| $ZnCl_2$ | 0.13 |
| $Se$ | 0.00025 |
| $I$ | 0.0009 |
| $MnSO_4 \cdot H_2O$ | 0.5 |
| $CoCl_2 \cdot 6H_2O$ | 0.1 |
| $CuSO_4 \cdot 5H_2O$ | 0.01 |
| $H_3BO_3$ | 0.01 |
| $Na_2MoO_4 \cdot 2H_2O$ | 0.03 |
| $NiCl_2 \cdot 6H_2O$ | 0.024 |
| $Na_2WO_4 \cdot 2H_2O$ | 0.025 |

- 250 mL of wastewater;
- 250 mL of medium containing
  - 245.6 mL of PBS solution;
  - 4.4 mL of vitamins and minerals solution;

The feeding solution was kept into a flask and heated through a thermostat bath (Julabo UC) at 37 °C (elevate temperatures accelerate the biofilm formation and improve the bioelectrocatalytic performances of the biofilm [14]) and bubbled with a continuous nitrogen flow (0.2 L/min, 1.013 bar, 23 °C) that keeps the cell environment anaerobic so the bacteria could oxidise the substrate and the counter reaction of oxygen reduction could take place on the cathode surface.
The flow rate of the inlet water was 0.07 mL/min (pump power: 5 rpm) a very low value chosen to assure a high Hydraulic Retention Time (more than 8 hours) at which bacteria had enough time to grow the biofilm on the anode electrode [7, 17].
The aim of the inoculation period was to let the bacteria acclimate to the cell environment so they stayed into the cell as long as possible (according to the continuous flow established for the experiment) hence they could colonize the electrode by producing the biofilm layer that assures the electrons generation. For this reason, in the start-up phase, the same solution containing both waste water and medium was recirculated into the cell passing through the heated flask which at the same time provided the inlet flow to the cell and received the effluent while being purged by nitrogen bubbling.
In this study no potential was applied to the electrodes (particularly the anode) of the first cell because of the risk of corrosion reactions but in other researches the anode potential was lowered to enhance the performance of the biofilm [9]. In the second cell after the inoculation period the anode potential was lowered by applying a negative voltage (-0.157 V vs. Ag/AgCl) to increase the cell voltage and acclimate the bacteria to lower potentials that assure better performances of the biofilm.
In order to monitor the biofilm generation on the anode electrode an Open Circuit Potential (OCP) measurement was carried out by setting the anode as working electrode and the cathode as counter electrode and collecting the data with a Potentiostat (Reference 600

™Potentiostat/Galvanostat/ZRA, Gamry Instruments) so it is possible to evaluate the cell voltage evolution over time in the start-up period. The OCP values were recorded every 10 min and the Voltage trend (vs. Ag/AgCl reference electrode) is shown in next chapter.
Some additions of glucose were necessary to assure a stable value of cell potential since an external source of carbonaceous substrate provides extra fuel to the bacteria colonies that need more nutrients in the growth phase: for this reason the feeding solution was amended twice with 1 g/L of D-(+)-Glucose (Sigma Aldrich) during the inoculation period.
The OCP monitoring was stopped when the cell voltage reached a stable value and a clear biofilm formation was visible but also an impedance analysis could certify the complete and stable formation of the anodic biofilm [6].

The second cell was acclimated as the first one with the same 1:1 ratio of wastewater and medium and at the same temperature and flow rate.
This time the biofilm formation was affected by external operations carried out in order to shorten the start-up phase: after one day of inoculation the electrodes were connected to an external circuit at high resistance (1000 Ω) but since the voltage increment was not appreciable the resistance was removed and the Open Circuit Potential was recorded until one week of inoculation and then a chronoamperometry procedure forced the system to achieve lower anode potentials that are recognised as more efficient for cell performances: the application of a potential to the anode electrode (-0.2 vs. SCE reference electrode) gave a more stable biofilm and a higher current production in other researches [9] so a final potential of -0.157 V vs. Ag/AgCl electrode was applied through the potentiostat in two different voltage step (first -0.07 V for 2 hours and then -0.157 V for 3.5 hours) to the anode which potential was 0.05 V vs. Ag/AgCl. The voltage trend during the start-up period and the results from the chronomaperometry test are shown in next chapter.

## 2.4 Analysis

After the inoculation and biofilm growing period the cells were fed with fresh solution both to provide new bacteria to the biofilm to stabilize it and to replace the substrates with new ones since the water loss was rather evident because of evaporation through the cathodes and inside the heated flask which supplied the inlet solution to the cell.
The ratio of waste water and medium was the same used in the inoculation test for mixed solution with both bacteria and medium:

- 250 mL of wastewater;
- 250 mL of medium containing
  - 245.6 mL of PBS solution;
  - 4.4 mL of vitamins and minerals solution;

The influence of different parameters is analysed by comparing various performances of the two cells in distinct operation conditions. Parameters switched and compared in the electrochemical tests are:

- flow rate, retention time;
- temperature;
- solution;
- time;
- cell type.

Retention time and temperature are tested in the variable resistance experiments on both cells and for the first cell two different solutions are inoculated in the cell: raw waste water and medium solution and an amended solution with waste water, medium and glucose as external organic fuel.
Time is a variable in power generation under removal conditions and both cells were connected to an external load during sampling the waste water treated by the cells and in the meanwhile current generated was recorded producing graphs current vs. time showed in next chapter.
Since most of these experiments were conduced on both cells an easy comparison of systems efficiency is possible to do.

### 2.4.1 Variable Resistance

Even if the use of the potentiostat would have been useful to determine the electrochemical processes of the cell, a less elegant and formal way of exploring cell performances was chosen by connecting the device to an external resistor and measuring the potential across the current collector with a multimeter.
A Decade Resistor Box (Swema) was used to change stepwise the external resistance: the three plugs in the box were used for the earth connection and for the cell electrodes through two alligators. The resistance could be changed from 0.1 to 1111 Ω and the different values used for the experiments are listed below (Tab. 2.5).
To record the cell voltage a Hewlett-Packard Multimeter (3468B) was connected with two plugs to the cell current collectors (titanium wires attached to the electrodes) and the voltage values were recorded every 20 min from the connection with the resistance.
The variable resistance test was conducted both with fresh solution (100 mL waste water, 98.24 mL phosphate buffer solution, 1.76 mL vitamins and minerals solution) and with the original solution amended with an organic compound: 1 g/L glucose for the first cell and with the amended solution for the second one.
The parameter switched in these tests were the hydraulic retention time and the temperature since they should be the most effective on power production. The different conditions tested are listed in Table 2.6 and the results obtained are reported in next chapter. For both the inlet solutions used three different conditions were analysed and particularly when the cell was fed with fresh solution the three tests were conducted in a row from the low retention time and low temperature, to high retention time and low temperature to the last one: low flow rate and high temperature. The cell was left under open circuit control for one hour between each test.
For the analysis with the amended solution (glucose addition) the data were recorded in two different days: the first day the temperature comparison test was performed and the next day the hydraulic retention time was switched between the two values to examine the cell behaviour. More than two hours under open circuit control were left to the cell between each experiment and this is the reason why the tests took two days.

The second cell polarization curves were obtained from data collected in the same day with the same procedure described above and with 2 hours of open circuit control between each operational condition. The tests were carried out using only the amended solution with glucose to enhance bacteria activity.
The external resistance values were switched from 1110 to 20 Ω so the system can be examined from the high load conditions (close to Open Circuit Potential) to the low load which involves low potentials. The highest external resistance (1110 Ω) was applied to explore the response of the cell at low current density were the activation losses are the controlling process so it is useful to see the voltage trend corresponding to high external loads (from open circuit to 700 Ω). Since Direct Current Voltage was recorded by the

multimeter the current values were calculated from voltage values thanks to Ohm law: $I = V/R$ and then cell power is also obtained from current and voltage as $P = IV$.
The step values of resistance used in the measurements are listed below and the corresponding voltage and current values are showed in the Result chapter and listed in the Appendix.

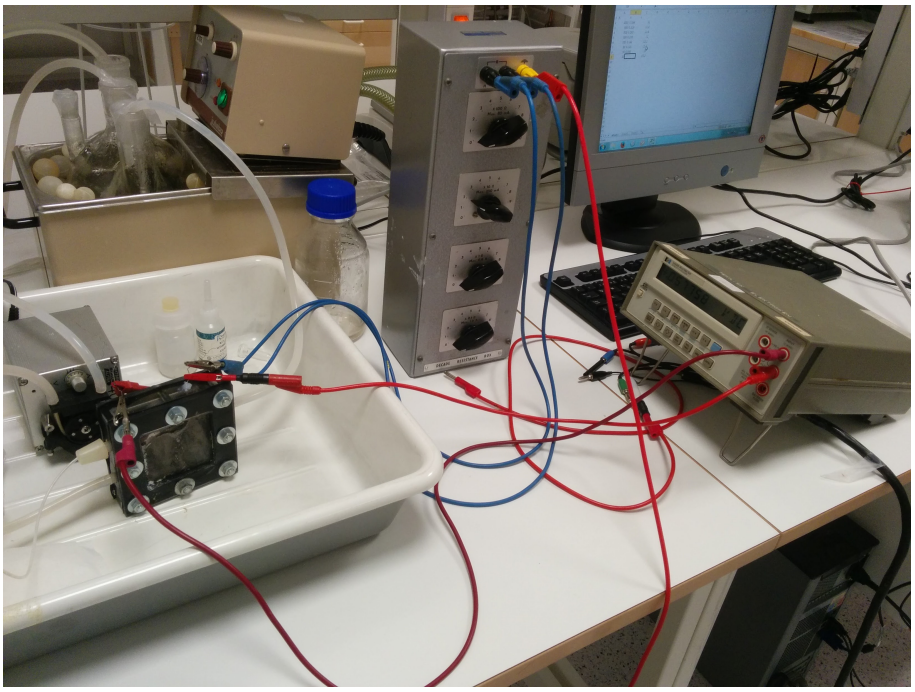

**Figure 2.10:** Variable Resistance Set-up

**Table 2.5:** External resistances steps

| R (Ω) | 1110 | 1000 | 700 | 400 | 100 | 80 | 50 | 20 |
|---|---|---|---|---|---|---|---|---|

**Table 2.6:** Variable resistance operational conditions

| Hydraulic Retention Time (h) | Temperature (°C) |
|---|---|
| 1.8 | 21.5 |
| 8.6 | 21.5 |
| 8.6 | 37 |

### 2.4.2 Cyclic Voltammetry

A cyclic voltammetry test was conducted to evaluate the anode electrochemical behaviour by using the Ag/AgCl electrode as reference, the anode as working electrode and the cathode as counter electrode all connected to the potentiostat (Gamry).
Following previous researches [22] the anode potential range was chosen between +0.2 and -0.6 V vs. Ag/AgCl and in order to explore a wider range of potential a second test was carried out changing the voltage range in -1,+1 V vs. Ag/AgCl and increasing the scan rate up to 10 mV/s.
Three cycles were obtained for every test and the third one is used to produce the plots reported in the next Chapter.

The parameters values used in the cyclic voltammetry test put into the Gamry Instruments software are listed below:

**Table 2.7:** Cyclic voltammetry parameters

| | First voltammetry | Second voltammetry |
|---|---|---|
| Initial Voltage | OCP | OCP |
| Scan Limit 1 | -0.6 V | -1 V |
| Scan Limit 2 | 0.2 V | 1 V |
| Final Voltage | OCP | OCP |
| Scan Rate | 1 mV/s | 10 mV/s |
| Step Size | 1 mV | 5 mV/s |
| Cycles (♯) | 3 | 3 |
| Max. Current | 100 mA | 100 mA |

The last cycle is also useful to plot the anode over-potential vs. log|current density| which can fit with a Butler-Volmer equation and that allows to determine the limiting step of the process. The first cyclic voltammetry set of data was chosen since a lower scan rate was applied and more data were available. The anode over-potential is taken from the positive voltage over the OCP and the corresponding currents were normalized over the cathodes area (A=0.0072 $m^2$).

The second cell was tested with a cyclic voltammetry as well and since it showed better connection between the anodic chamber and the reference electrode the results obtained with this cell appear to be more reliable.
The same features of the first CV performed on the first cell were used in this case: the anode potential was varied from -0.6 to +0.2 V vs. Ag/Ag/Cl and the scan rate was fixed at 1 mV/s to collect more data.
Either the anode and the cathode electrode were investigated by switching them as working and counter electrode on the potentiostat clamps (Tab. 2.8). These plots are useful to

**Table 2.8:** Cyclic Voltammetry parameters of second cell with anode or cathode as working electrode

| Working electrode: anode | | Working electrode: cathode | |
|---|---|---|---|
| Initial Voltage | -0.132 V (vs. Ag/AgCl) | Initial Voltage | 0.34 V (vs. Ag/AgCl) |
| Scan Limit 1 | 0.2 V (vs. Ag/AgCl) | Scan Limit 1 | -0.15 V (vs. Ag/AgCl) |
| Scan Limit 2 | -0.6 V (vs. Ag/AgCl) | Scan Limit 2 | 0.6 V (vs. Ag/AgCl) |
| Final Voltage | -0.132 V (vs. Ag/AgCl) | Final Voltage | 0.34 V (vs. Ag/AgCl) |
| Scan Rate | 1 mV/ | Scan Rate | 1 mV/s |
| Step Size | 1 mV | Step Size | 1 mV |
| Cycles (♯) | 2 | Cycles (♯) | 2 |
| Max. Current | 100 mA | Max. Current | 100 mA |

evaluate the reactions limiting factors and from the same set of data other curves can be obtained: voltage trend vs. logarithm of current density and voltage vs. current for both electrodes which is representative of the cell potential as the difference between cathodic and anodic potentials is the total cell voltage.

### 2.4.3 Open Circuit Voltage monitoring

The first cell was run for more than one month and after the incubation and growth period above described the Open Circuit Potential between the anode and the two cathodes was

recorded every day and the cell was fed with an external organic addition of 1 g/L of glucose every day.
The OCP data were obtained from the Gamry potentiostat by short circuiting the reference plug with the cathode one or from the multimeter in which only two alligators were used for the two electrodes.
In the following chapter the trend of cell OCP is reported in a graph to determine the autonomy of the cell and its life-cycles between one fuel addition and the next one.

### 2.4.4 Substrate removal

Biological analysis were performed on both cells varying the Hydraulic Retention Time of waste water in the devices. The inflow solution was composed exclusively by waste water without medium or other additions. The contents of the cells previously used for the inoculation phase and electrochemical tests was removed since the original waste water was mixed with the medium solution. To do that the waste water was injected into the cell and the out flow liquid was disposed. After 72 mL of outflow solution were expelled, the cells were considered filled with only waste water and the experiments started.
The different Hydraulic Retention Times used during the samplings are listed in Tab. 2.9 and the cells were also connected to the external resistor with 100 Ω load because at this value the device is capable of producing the highest power so for a perspective of real application this value appeared more interesting.
For the second cell also a test with the Open Circuit control was performed since in that case the COD removal is supposed to be lower [21]. The samples were analysed with WTW

**Table 2.9:** Substrate removal analysis conditions

| Operational conditions | First Cell | | Second cell | | |
|---|---|---|---|---|---|
| Hydraulic Retention Time (h) | 8.6 | 1.8 | 8.6 | 1.8 | 1.8 |
| External load (Ω) | 100 | 100 | 100 | 100 | Open Circuit |

(a xylem brand) cuvettes either for the COD and total nitrogen by using a thermoreactor (CR 4200 WTW) and a photometer (*photoLab* 6600 UV-VIS series).
The COD (Chemical Oxygen Demand) express the amount of oxygen originating from potassium dichromate that reacts with the oxidizable substances contained in 1 L of water under the working condition of the specified procedure.
1 mol $K_2Cr_2O_7$ is equivalent to 1.5 mol $O_2$. The results are expressed as mg/L COD (=mg/L $O_2$).
The water sample is oxidized with a hot sulfuric solution of potassium dichromate, with silver sulfate as the catalyst. Chloride is masked with mercury sulfate. The concentration of green $Cr^{2+}$ ions is then determined photometrically.
This test measures organic and inorganic compounds oxidizable by dichromate. Exceptions are some heterocyclic compounds (e.g. pyridine), quaternary nitrogen compounds and readily volatile hydrocarbons.
The cells containing the reactants were swirled to suspend the bottom sediment and then 3 mL of each sample were injected into all of them. The content of the cell was vigorously mixed again and afterwards the reaction cells were heated for 120 min at 148 °C in the thermoreactor.
After reaction time they were removed from the thermoreactor and allowed to cool in a test-tube rack. A cooling time of 30 min was necessary before final analysis took place. The cells were wiped to avoid to affect the measurements with dirt on the glass.

Organic and inorganic nitrogen compounds are transformed into nitrate according to

Koroleff's method by treatment with an oxidizing agent in a thermoreactor. In a solution acidified with sulfuric and phosphoric acid, this nitrate reacts with 2,6-dimethylphenol (DMP) to form 4-nitro-2-6-dimethylphenol that is determined photometrically.
An empty cell was filled with 1 mL of each sample, 9 mL of distilled water were added with one microspoon (1 level) with Reagent N-1K and 6 drops of Reagent N-2K. The cells were mixed and put in the preheated thermoreactor for 1 hour.
They were let cooling at room temperature for 30 min in a test-tube rack and were shaken to prevent turbidity and precipitation to alter the results. The following step was preliminary to the measurement: 1 mL of the digested, cooled sample was pipetted into the reaction cell (the supernatant solution was sucked to avoid precipitate and turbidity) and 1 mL of Reagent N-3K was added with a pipette as well and the cell became hot because of the reaction. The reaction time is approximately 10 min so the cells were let to stand for this time and then they were cleaned before putting them in the photometer to not interfere with the absorbance values.

From the values of COD in the effluent coulombic efficiency can be calculated to evaluate the efficiency of exoelectrogens bacteria since the higher the coulombic efficiency the more active the exoelectrogenic bacteria are: different microorganism colonies are contained in the water and both aerobic and anaerobic bacteria are involved in substrate consumption but as only the anaerobic bacteria that can transfer the electrons produced in the nutrient oxidation to the anode electrode are involved in current generation, the coulombic efficiency is a way to detect which bacteria colony has developed more into the chamber.
During the sampling for the COD test the cell was connected to the potentiostat that recorded the current generated over time and this set of data is necessary to calculate the integgral at numerator in coulombic efficiency equation (2.2).
The constant parameter is assumed to be 8 for COD since it represents the oxygen molecular weight ($M_s = 32$ g/mol) over the electrons involved in COD removal (4), the Farady constant is 96485.333 C/mol and the cell internal volume is 36 $cm^3$.

$$C_E = \frac{M_s \quad \int_0^t I\,dt}{F \quad b_{es} \quad \nu_{An} \quad \Delta COD} \tag{2.2}$$

The values of substrates obtained from the photometric analysis are used to estimate the removal efficiency of the device calculated as

$$\eta_S = \frac{[S]_0 - [S]_f}{[S]_0} \times 100 \tag{2.3}$$

where $[S]_0$ is the substrate initial concentration (mg/L) and $[S]_f$ is the final concentration measured from the samples taken at different times.
The removal rate can be another interesting parameter of cell removal performances and it is calculated as

$$r_S = \frac{[S]_0 - [S]_f}{HRT} \tag{2.4}$$

since different hydraulic retention times were tested the removing time is assumed as the retention time (HRT) for each experiment.

From the same samples the pH was analysed in order to detect the reactions occurring in the cell that can induce protons consumption or production and hence a pH change in the effluent water.
A pH-electrode (SenTix 41, WTW) was immersed in the samples solutions and the pH value was read on the display connected to the electrode after a couple of minutes required to obtain a stable value.

# Chapter 3

# Results and discussion

## 3.1 Anode characterization

From the SEM images of the anode electrode it is possible to compare the original commercial vitreous carbon foam and the one treated with nitric acid.
The main aim is to understand if the porous structure of the foam got benefits from the acidic treatment and if the surface increased.
The treated foam looks rougher at a first sight even if the difference is not so evident.
Using a higher magnification (Fig. 3.1c and 3.1d) it is possible to observe a rougher surface of the treated foam that is still quite flat so the treatment gave good results but could be not so impressive.
The last pictures (Fig. 3.1e and 3.1f) show the smallest pores in the range of $\mu m$ that is the most interesting size as generally bacteria dimensions are about 0.3 $\mu m$. The treated foam hosts more pores of different dimensions and even if there are no pores as small as a microorganism it is good to have a bigger surface for bacteria colonies.
The acidic treatment at the end could have been positively effecting but the foam area still appears not completely homogeneous and evenly porous: the high porosity at microscopic dimensions and the bigger sizes of exoelectrogens bacteria compared to other heterotrophic microorganisms can permit to conclude that the anode electrode was potentially a good environment for biofilm formation.

The BET analysis data were plotted (Fig. 3.2) according to linearized equation to obtain the parameter characteristic of the material: the surface area.
Only the treated foam gave reasonable value while the untreated one reported an error too high to consider the result acceptable.

**Table 3.1:** Linearized BET equation parameters

| | |
|---|---|
| BET surface area | $1.9537 \pm 0.0768 \quad m^2/g$ |
| Slope | $2.2333 \pm 0.0867$ |
| Y-intercept | $-0.0052 \pm 0.0122$ |
| C | $-431.6127$ |
| $V_m$ | $0.4488 \quad cm^3/g$ |
| Correlation coefficient | 0.9955 |

Simultaneously the instrument recorded the BJH absorption data that are useful to better understand the pore size distribution of the material. Some features are listed in Table 3.2. Since the BET analysis gives the surface area per gram of electrode (1.954 $m^2/g$) it is possible to determine the total area of the carbon foam: the two layers used as electrode were heavy 1.82 g so the total surface area of the foam was 3.556 $m^2$ which is a promising

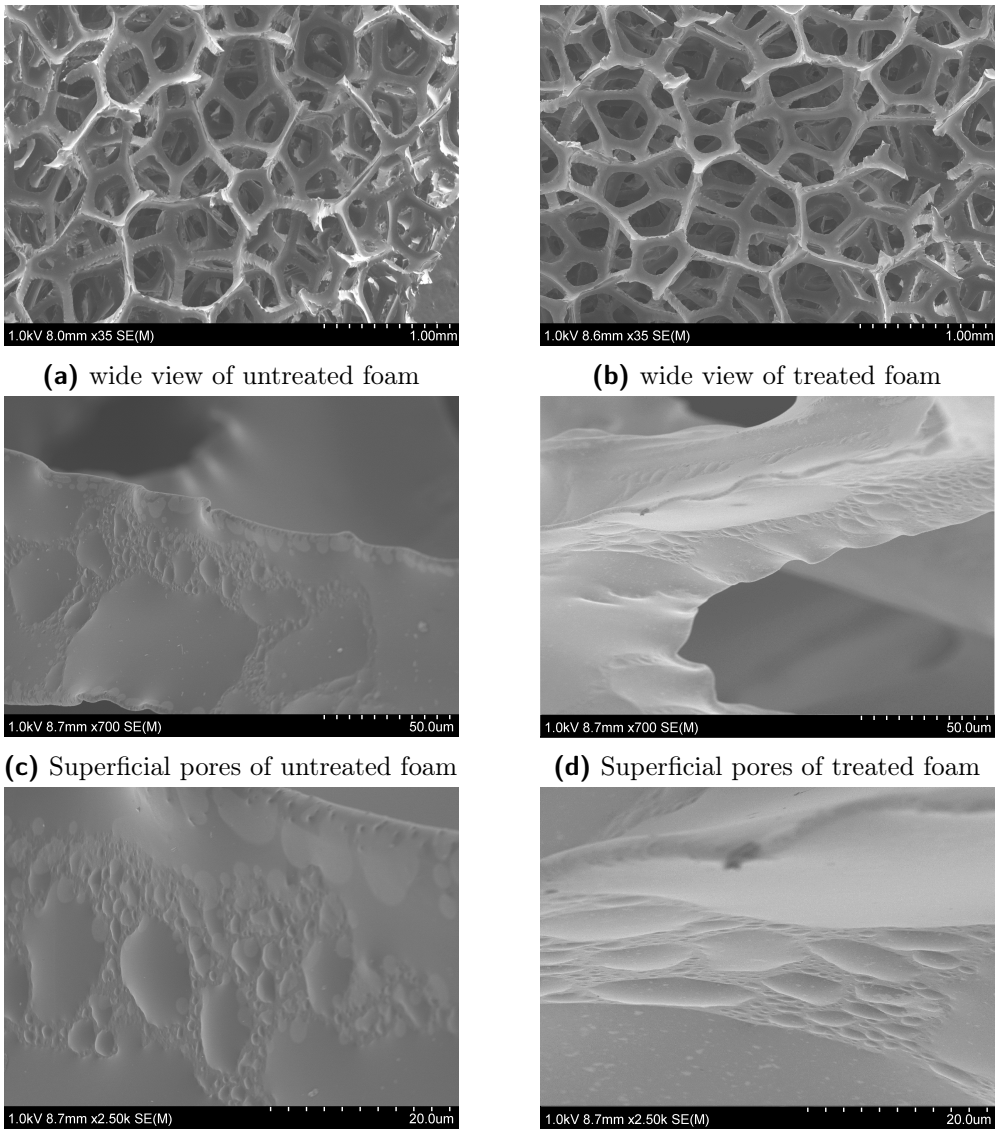


**(a)** wide view of untreated foam

**(b)** wide view of treated foam

**(c)** Superficial pores of untreated foam

**(d)** Superficial pores of treated foam

**(e)** wide view of untreated foam

**(f)** wide view of treated foam

**Figure 3.1:** External views comparison of untreated and treated foams

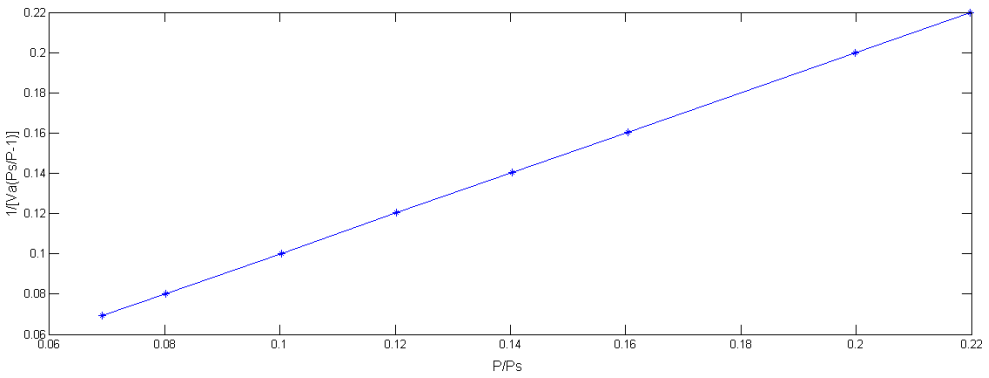


**Figure 3.2:** Linearized BET equation graph

value for an electrode which has to host bacterial colonies.
However the geometrical anodic area was used to refer to current density for electrochemical

**Table 3.2:** BJH pore distribution

| | |
|---|---|
| Diameter range | 17 to 3000$\mathring{A}$ |
| Adsorbate Property Factor | 9.53$\mathring{A}$ |
| Density Conversion Factor | 0.001547 |
| Fraction of pores open at both ends | 0 |

results.

## 3.2 Cathode realization

The second type of cathodes (activated carbon catalyst) were manufactured in order to use them in the second cell and compare their performance with the other catalyst used in the first cell (cobalt). Several attempts were made in order to follow accurately the recipe [20] but after the phase inversion step the electrodes were let drying in the fume hood and after few hours they started to crack on the outer surface so a last try was made by putting the electrodes into water overnight and taking them out of water only before using them in the cell so the drying step was postponed. The electrodes showed cracking issues both when the slurry was spread with a spatula by hand and when they were afterwards pressed by the calender. The electrodes after the phase inversion step are still smooth and uniform while in Fig. 3.3 the previous attempts made with cathodes dried in the fume hood are shown and the cracks on the surface are evident even if putting them into water seems to let the polymer expand a bit again and reach the original shape.

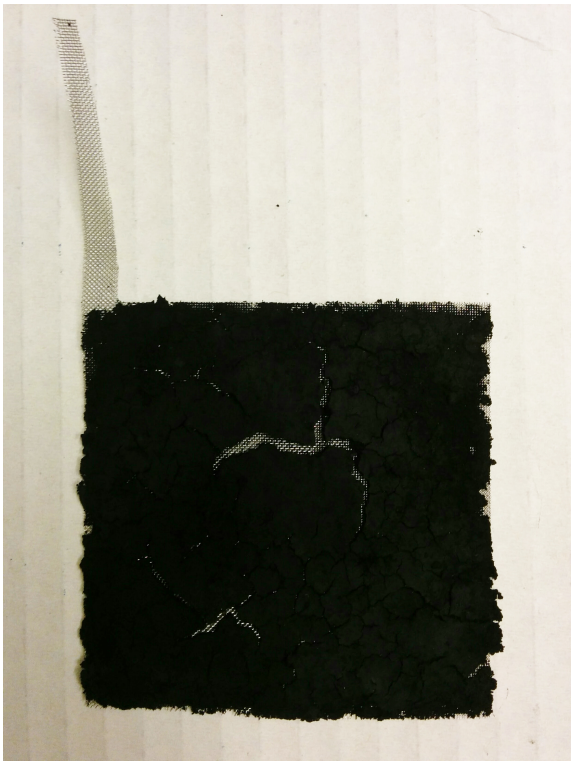

**Figure 3.3:** Cathode electrode showing cracks after drying

The catalyst layer has to face the air side since it works as a diffusion layer as well and it catalyses the oxygen reduction reaction in gas phase in which its percentage is higher than in water. The cathodes manufactured were used in the cell but they ended in leaking

water because of cracks on their surfaces, so another kind of electrode was fabricated with a different method and different reactants.
This kind of electrodes seems promising for this application for the low cost and the idea of mixing the active and diffusion layer to catalyse the reaction in the gas phase but apparently the composition and ratios reported in the paper are not suitable for such a big electrode as the ones fabricated in this work.
For reproducible electrodes with active and diffusion layer a more accurate solvent removal seems to be necessary (for the other electrodes both thermal treatment and mechanical pressure were used to get rid of the solvent) to get a uniform electrode surface and avoid cracks that can affect the activity of the electrode or in the worst scenario can conduce to water leakage.

## 3.3 Inoculation and biofilm growth

From the inoculation phase it is possible to evaluate the biofilm growth by monitoring the voltage trend over time (Fig. 3.4) since the bacteria deposited over the anode electrode surface are responsible for the electrons generation which induces the voltage changes on the electrode. According to Fig. 3.4 the voltage value is quite stable and it shows a positive

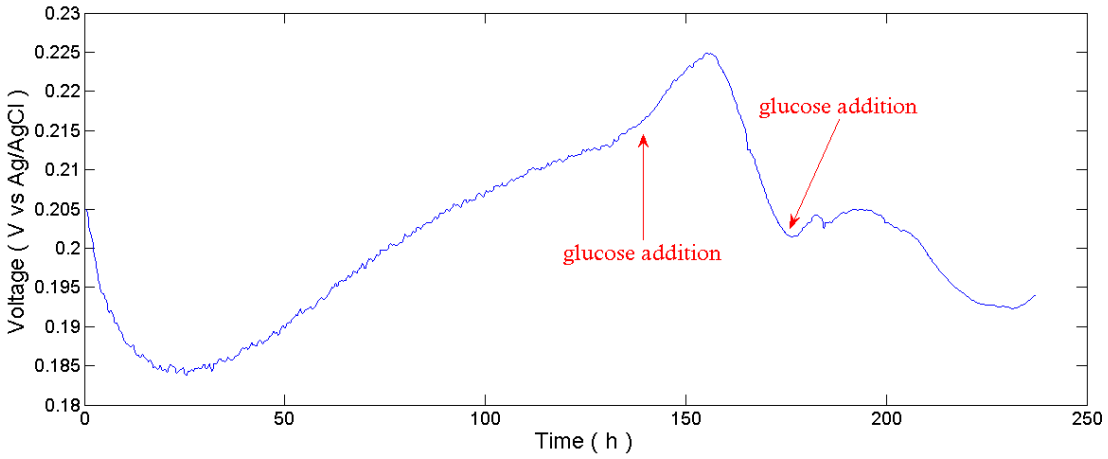


**Figure 3.4:** Open Circuit Potential (vs. reference electrode Ag/AgCl) during cell's start-up: Biofilm formation is related to voltage trend and the two peaks after fuel addition (glucose) are likely due to substrate consumption by two different bacteria families

peak after a lag period in which the OCP decreases (likely due to bacteria acclimatization). After 5 days (122 h in the graph) 1 g/L of glucose was add to provide more fuel to the cell in terms of substrate for the microorganism. This is the reason of the higher increase in voltage before the first peak and similarly before the second peak other fuel was put into the cell with the same concentration.
According to previous researches [15] two different voltage peaks could be caused by two primary groups of bacteria inside the cell. The first peak is likely generated by the suspended bacteria which are faster in consuming simple substrates growing at a higher rate than others species. The second peak is hence related to the aggregated bacteria that live in colonies on the biofilm layer developed on electrode walls. The former are less important in the current generation since the main quantity of electricity produced in the device comes from the biofilm bacteria.
To evaluate the biofilm growth via electrochemical measurements it is possible to refer to voltage trend and assume the growth complete when a stable potential is obtained: in this case it seems that after 10 days the values are pretty close to each other even if an anodic

impedance spectroscopy and a microscopy analysis could be more reliable ways of detection. The strict dependence of biofilm growth with temperature is outlined by Patil [14], in fact in this study the lag time of a microbial fuel cell run at 22 °C resulted 290 h (∼ 12 days) while at 35 °C the biofilm growth took 85 h (∼ 3.5 days). The third temperature tested is the average temperature of Waste Water Treatment Plants in Europe (15 °C) led to a lag time in biofilm complete formation of more than 40 days. The mesophilic character of the exoelectrogenic bacteria is far more clear from the monitoring of biofilm formation at 5 °C that was observed after more than 2 months.

The second cell start-up phase was characterized by the application of an external resistance after the lag period of biofilm acclimation and the chronoamperometry to stabilize the anode to lower potentials to which corresponds a high current generated. In Fig. 3.5

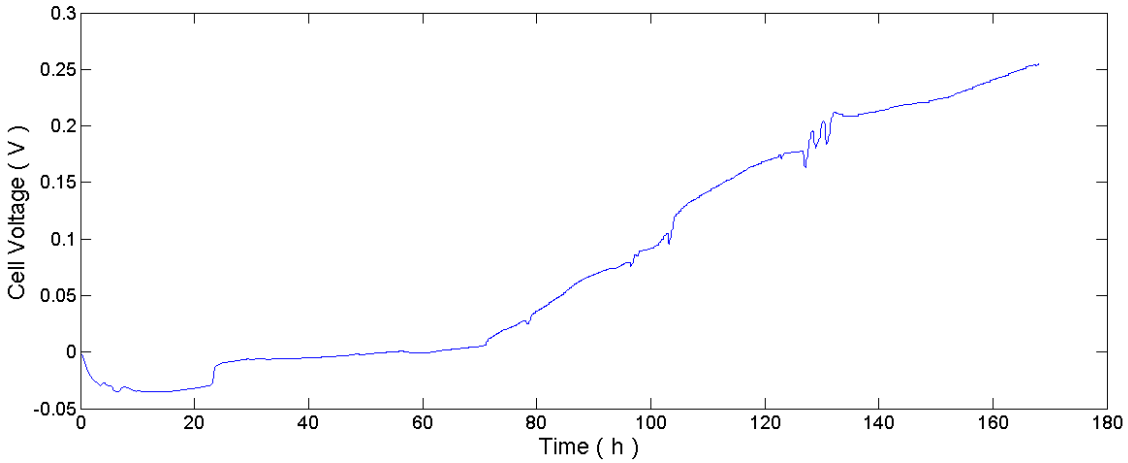


**Figure 3.5:** Open Circuit Potential during cell start-up: after the lag period the cell was connected to an external resistance for 54h and run at Open Circuit Potential afterwards

the cell voltage over time in the inoculation period is reported and it is appreciable the lag time of about one day (negative cell potentials) in which the bacteria colonized the electrode and start to produce electrons and the flat curve corresponding to the application of the external load to the circuit which did not favour a fast increment of cell potential that is though visible after 75 h onwards. After one week of operation the cell potential

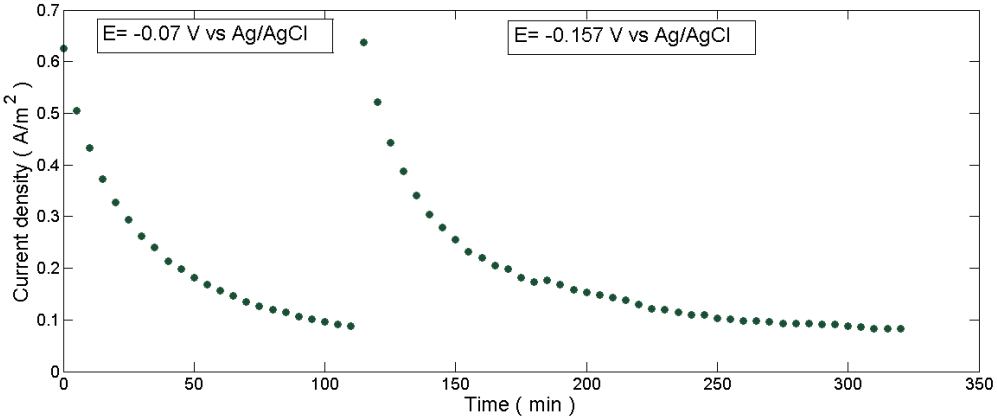


**Figure 3.6:** ChronoAmperometry on the second cell: two step size were applied and the corresponding current was recorded over time

reached 0.25 V and the chronoamperometry applied on it for one day helped to increase

the OCP of the cell which was 0.52 V the day after.
From the curves obtained (Fig. 3.6) it is evident that at lower potential the biofilm was not enough acclimated and the current decay was faster but it was able to maintain a stable current value (even if low) over time. The following day, after 17 h of Open Circuit control, the anode potential was -0.12 V vs. reference which means that the biofilm was more stable at low potential and it positively affects cell voltage since it reached an OCP of 0.52 V with such a anode potential. The electrodes voltage trend during biofilm development for the

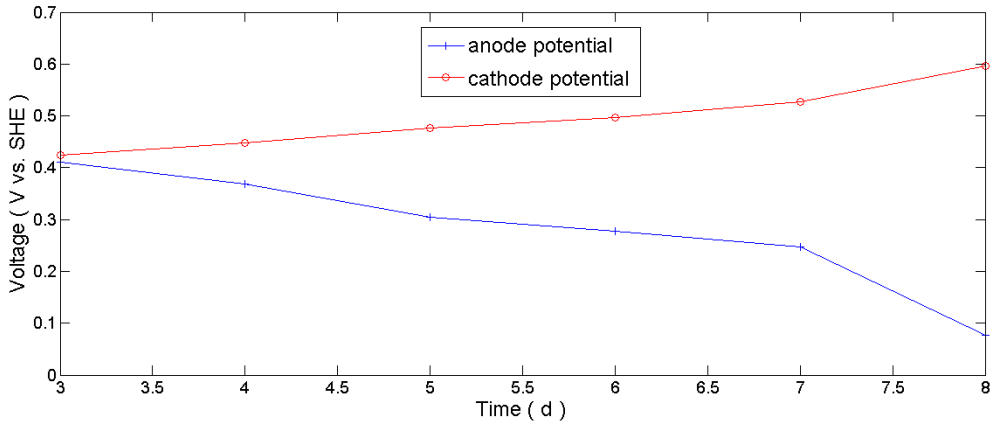


**Figure 3.7:** Electrodes potentials of the second cell during biofilm formation: anode voltage decrease due to bacteria activity and cathode increase lead to higher cell voltage

second cell is reported in Fig. 3.7: the anode potential decreased because of bacteria activity and subsequently the cathode electrode received more reactants (protons and electrons) for the counter reaction.
The anode voltage progressively decreased until day 8 when the chronoamperometry test was conduced and the potential was forced to reach low values (0.04 V vs SHE) hence the counter reaction was enhanced and the cathode potential rose up to 0.6 V vs SHE.

## 3.4 Open Circuit Voltage monitoring

The Open Circuit Potential of the first cell during one month of operations is shown in Fig. 3.8 from which it is possible to evaluate the cycle times of the cell, that in other studies [22] are defined as the time span between adding fresh medium in the cell (run under batch conditions) and the voltage drop to <50 mV. In this case the cell solution was enriched with glucose every day and the cell voltage never decreased to such a low value but from the graph reported it is evident that when the time span between each addition is bigger than one day (typically 3 days between each inoculation were reached during the weekend) the voltage drop is more consistent than normal trend.
It is also important to notice that from the first record the cell voltage decreased constantly during the monitored period and that could be due to the efficiency of cathode electrode that was probably affected by salt depositions on its surface and corrosion reactions that can have a strong influence on the cathodic over-potential since nickel electrode potential is 0.257 V under standard conditions but in any case it can be a reason of the voltage decrease during time in the cell. In fact as shown in next section, the cathodes surfaces presented green spots that are most likely due to nickel oxide deposition.
Another reason of the lost of efficiency can rely on the formation of carbon dioxide in the anodic solution: from the Plexiglass chamber it is possible to see that the cell is not completely full and some gas bubbles are trapped on the top of it: that can diminish the anode surface available for the reaction.

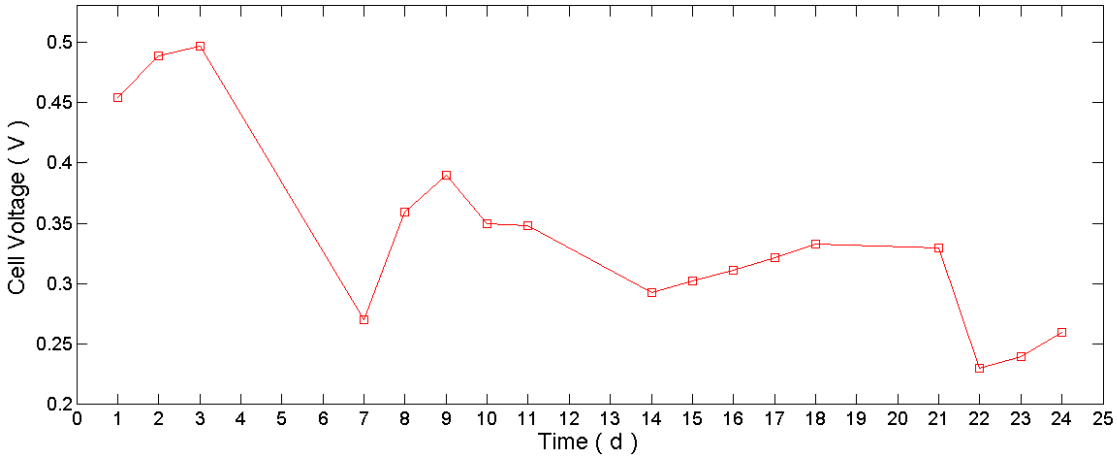


**Figure 3.8:** Open Circuit Potential over time

## 3.5 Electrochemical performances

Effects of different parameters tested in the experiments (retention time, temperature, type of solution, time) are reported in several graphs in order to compare the performances of both cells in variable operational conditions.
Flow rate and temperature are analysed through polarization and power density curves obtained in the variable resistance test for both cells and the influence of different solutions is also examined on the first cell.
Variable efficiency over time is observed through the current record during removal analysis for the two cells.
Cyclic voltammetry curves are useful to investigate electrodes behaviour: only anode was tested in first cell cyclic voltammograms while both anode and cathode were studied by scanning the electrode potential in the second cell.

### 3.5.1 Variable resistance

By connecting the cell to an external resistance polarization curves can be obtained: in these plots the cell potential is represented and the current extracted is calculated from the Ohm law: $I = V/R$ where external resistance is fixed by the resistor and switched every 20 minutes and the voltage is recorded by the multimeter.
The same resistance values were used for all the tests hence all current and power values were calculated from the voltages recorded during the experiments.
The main goal of a MFC is to produce a high power density meaning that a great current value corresponding to maximum potential is desirable. Even if in this case very low power densities are reached, the significant result obtained by the power density plots is that as other studies confirms [21] the maximum power generated corresponds to an external load of 100 Ω.
From the polarization curve (cell voltage vs. current density, Fig. 3.9b, 3.10b, 3.11b, 3.12b, 3.13b, 3.14b) it is possible to evaluate three different potential losses: at low current density there is a rapid voltage loss subsequent to the connection to the external load after the Open Circuit Potential control, the reason of this loss should rely on the activation loss of bacteria that consume energy in the release and transfer of electrons. In the linear part a constant voltage drop is due to the ohmic loss and at high current densities another rapid voltage drop is observed and this region is interesting because it is been demonstrated that MFC acclimated under low external resistances are more efficient [5] so they achieve higher cell voltage and subsequently greater current densities.

From polarization curves and power density curve is possible to compare the performances of a cell under different conditions: in this case the first cell was run with a low flow rate that produces a high Hydraulic Retention Time (8.6 h) and with a lower HRT (1.8 h) and it was also tested at high and room temperatures at the same retention time.
These tests were made by feeding the cell with the waste water and the medium (1:1 ratio) and by amending this solution with an extra fuel (1 g/L glucose).
Same tests were carried out on the second cell fed with an amended solution containing 1 g/L of glucose.
All data recorded and calculated represented in these plots are listed in Appendix.

**First cell fed with raw waste water and medium solution**

In Fig. 3.9 the performances of the cell fed with fresh solution (the only fuel provided to the cell comes from the organic matter contained in the waste water) under different retention times are shown.
It is important to underline that the data of the higher flow rate were collected before the others and 2 hours under Open Circuit control were left to the cell to stabilize after the first experiment. This is the reason why the Open Circuit Potential of the first experiment is higher but then an evident drop in voltage brings to lower values than the other condition in which hence the cell seems to be more efficient and this is more appreciable from the power density graph (Fig. 3.9c) where the power density is higher under higher retention time condition and it also shows a good performance with low external load: the last datum is characterized by a surprisingly high cell voltage so the cell is quite well acclimated at low resistances.
What is more interesting is the power overshoot occurring at a low retention time: according to other researches this problem could be attributed to mass transport limitations, electrical and ionic depletion on the anode at low external resistances, substrate utilization, age of the anode biofilm, extreme operating conditions, and insufficient acclimation time for microbes to adjust to a new resistance or a rapid change of voltage. The last one seems to be the more reliable since it is been demonstrated that "acclimating reactors to the low external resistances eliminated power overshoot and allowed the biofilm to achieve increased current densities as the anode potential increased" [5].
Anyway the power overshoot is referred to anode performance and not to the cathode which was quite affected by salt deposition on its surface so the active area should have been diminished even though it was not the limiting step of the cell power production.
Temperature effect is analysed by observing Fig. 3.10 and the anomalous behaviour of the system at higher temperature that should guarantee better performances in current and power generation can be adduced to the polarization effect of the cell since the test at higher temperature was carried out later than the low temperature and the cell seems to show higher efficiency at the beginning of the experiment when more fuel is contained in the solution and the effect of the external load that withdraws electrons from the biofilm is less evident and then probably the microorganisms cannot produce enough charge to sustain the circuit load.

**First cell fed with raw waste water and medium solution amended with glucose**

The second polarization tests were obtained from the first cell fed with the solution amended with co-substrate (glucose 1 g/L) and the same conditions explored in the first test were analysed. Other polarization and power density curves are plotted from the data recorded and it is interesting to notice that the results are different from the first test.
The most probable reason is that the order of the different conditions was changed and the cell showed better results for the first experiment of every polarization test, this can be due

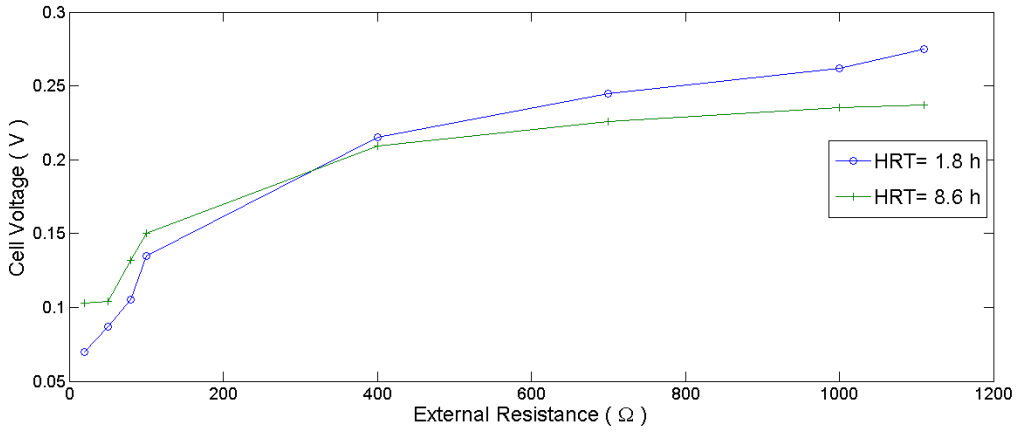


**(a)** Cell voltage recorded by switching external load values

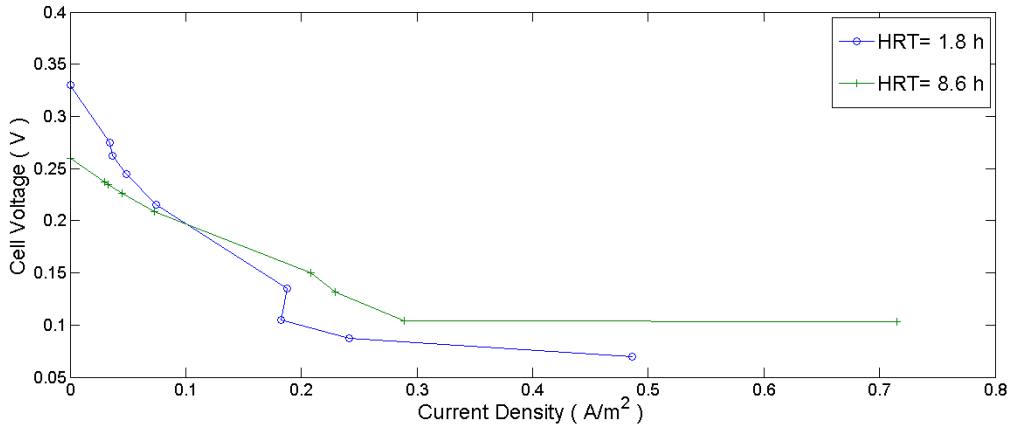


**(b)** Polarization curves: cell voltage vs. current density normalized by cathodes area (72 $cm^2$)

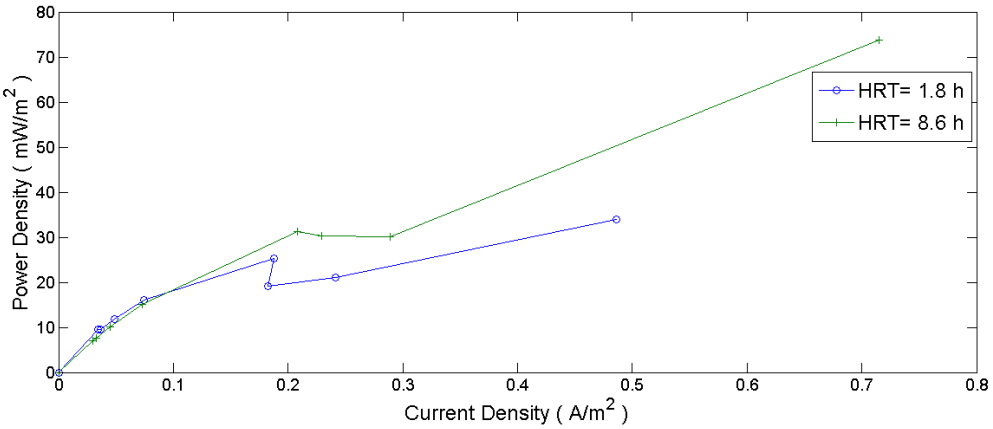


**(c)** Power density curves: power density and current density referred to cathodes area (72 $cm^2$)

**Figure 3.9:** Electrochemical performances comparison at different retention times for the first cell fed without an external organic fuel

to the higher quantity of fuel present in the solution at the beginning of the day as well as to the polarization effect of the cell which was normally run under Open Circuit control and after several hours of closed external circuit lost its efficiency. The only visible effect of different operational conditions is the increase of the cell voltage at high temperature (the

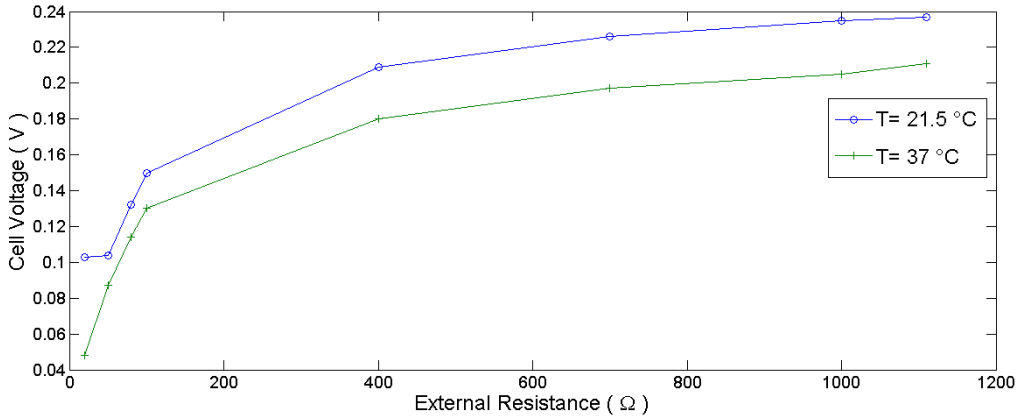


**(a)** Cell voltage recorded by switching external load values

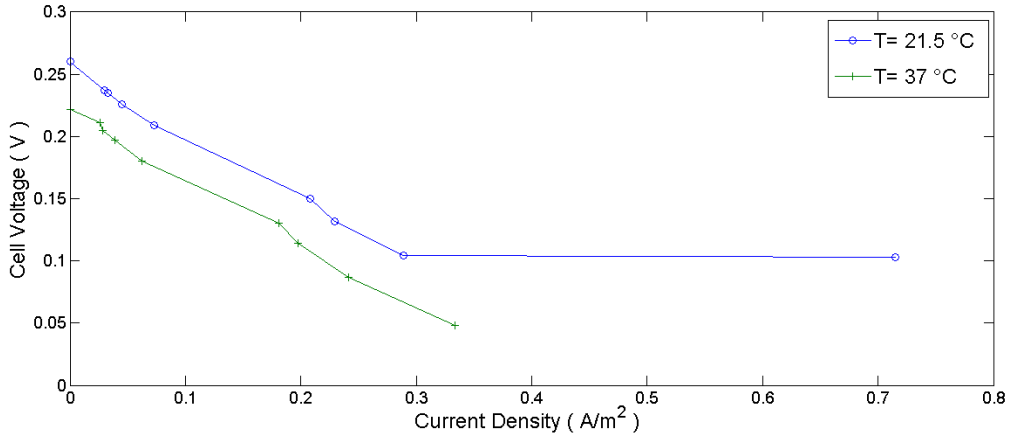


**(b)** Polarization curves: cell voltage vs. current density normalized by cathodes area (72 $cm^2$)

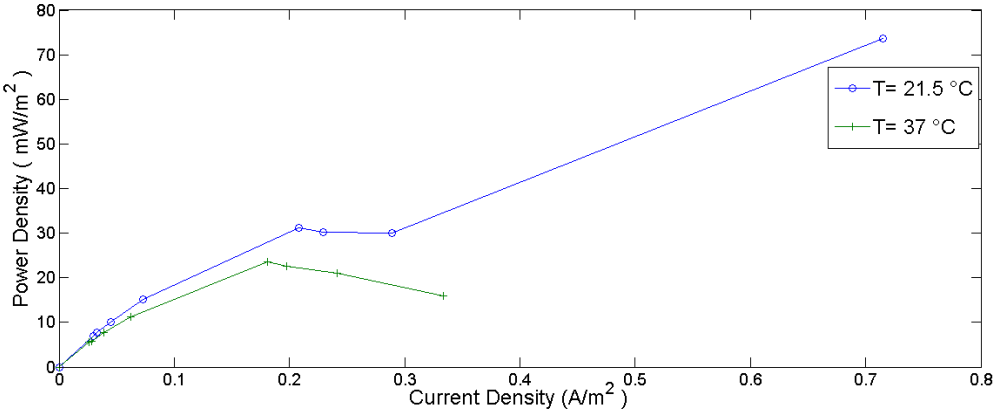


**(c)** Power density curves: power density and current density referred to cathodes area (72 $cm^2$)

**Figure 3.10:** Electrochemical performances comparison at different temperatures for the first cell fed without an external organic fuel

OCP rose from 0.26 V to 0.38 V) but it suddenly dropped when connected to the external resistance and actually it scarcely overtakes the cell voltage at lower temperature which showed a slighter decrease at lower external loads.
The anomalous behaviour of the cell at high temperature in the potential range close to the OCP reflects also on the power density curve that shows a potential overshoot whose

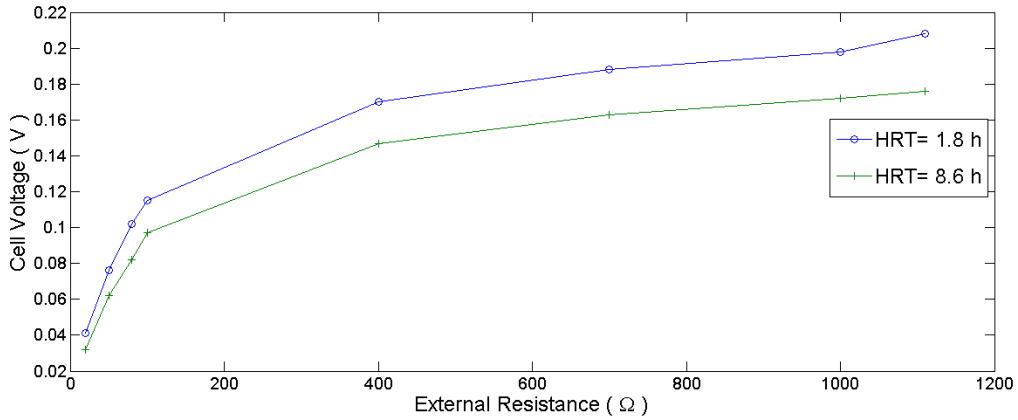


**(a)** Cell voltage recorded by switching external load values

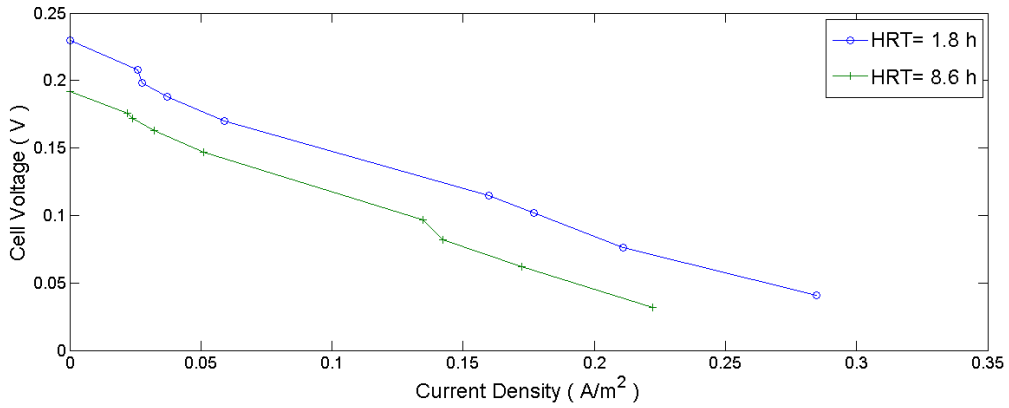


**(b)** Polarization curves: cell voltage vs. current density normalized by cathodes area (72 $cm^2$)

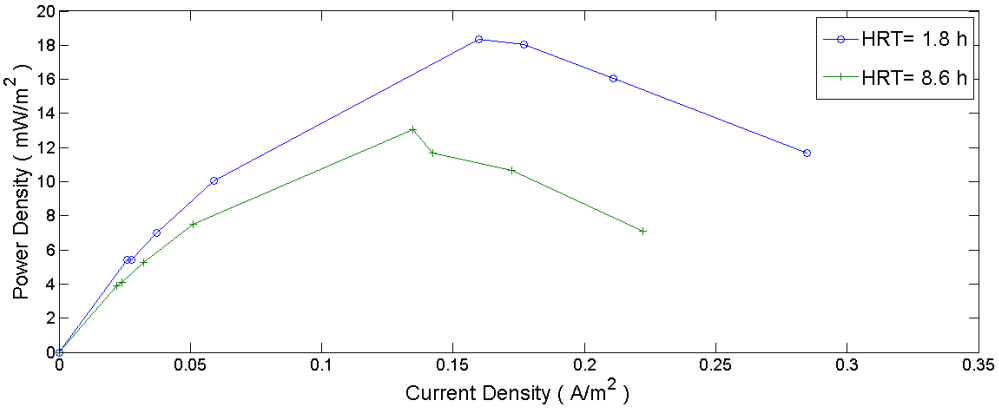


**(c)** Power density curves: power density and current density referred to cathodes area (72 $cm^2$)

**Figure 3.11:** Electrochemical performances comparison at different retention times for the first cell fed with an external organic fuel

reason is likely the temporary disturbance of biofilm that enhanced its enzymatic reactions but not the efficiency of the system.

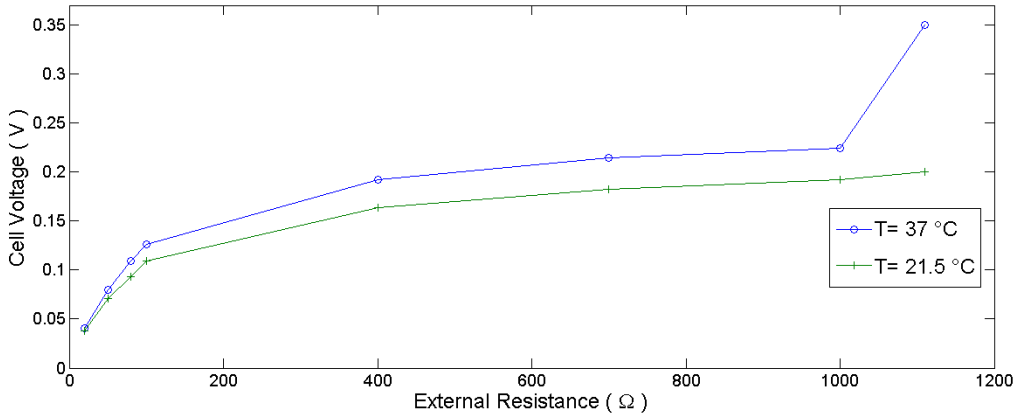


**(a)** Cell voltage recorded by switching external load values

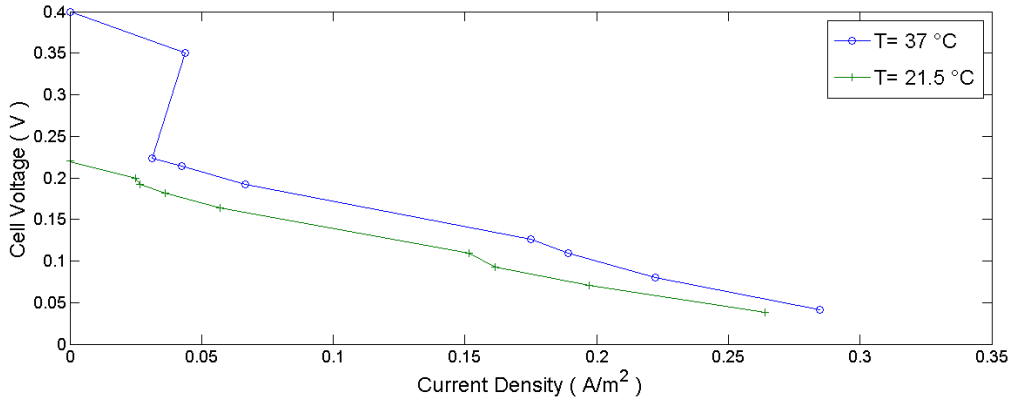


**(b)** Polarization curves: cell voltage vs. current density normalized by cathodes area (72 $cm^2$)

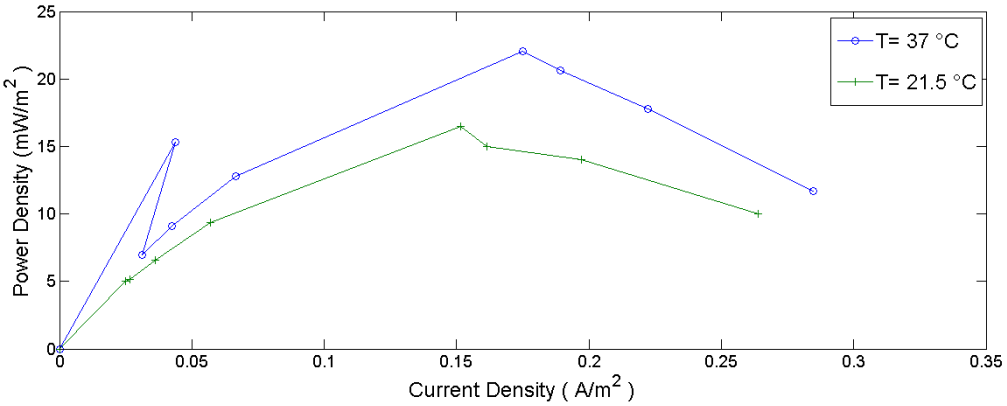


**(c)** Power density curves: power density and current density referred to cathodes area (72 $cm^2$)

**Figure 3.12:** Electrochemical performances comparison at different temperatures for the first cell fed with an external organic fuel

### Second cell fed with raw waste water and medium solution amended with glucose

The second cell was tested with the variable resistance technique after two weeks of start-up and even if the biofilm was not completely stabilized the results achieved by the cell look promising.
The same operational conditions of the first cell were tested and the solution used contained

1 g/L of extra fuel (glucose) and in Appendix the cell voltages recorded by the multimeter at different external loads are listed and from them the corresponding currents and power produced are calculated. For this cell the different operational conditions seem to slightly

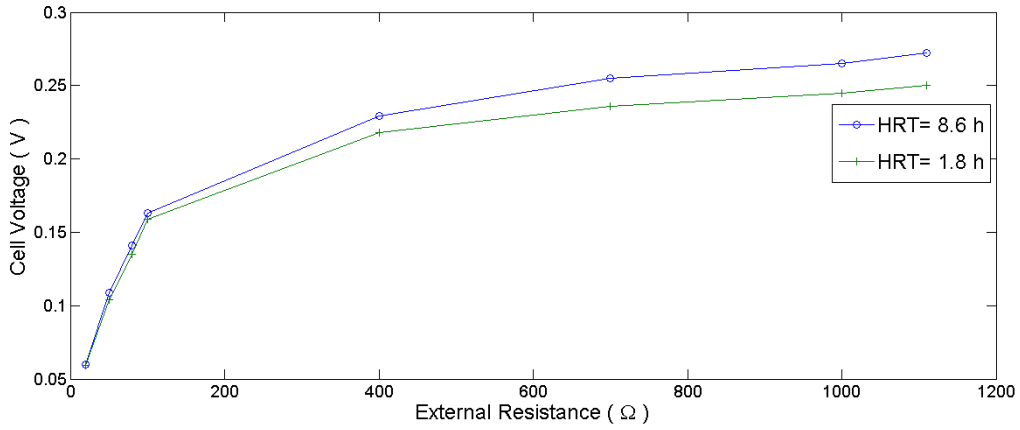


**(a)** Cell voltage recorded by switching external load values

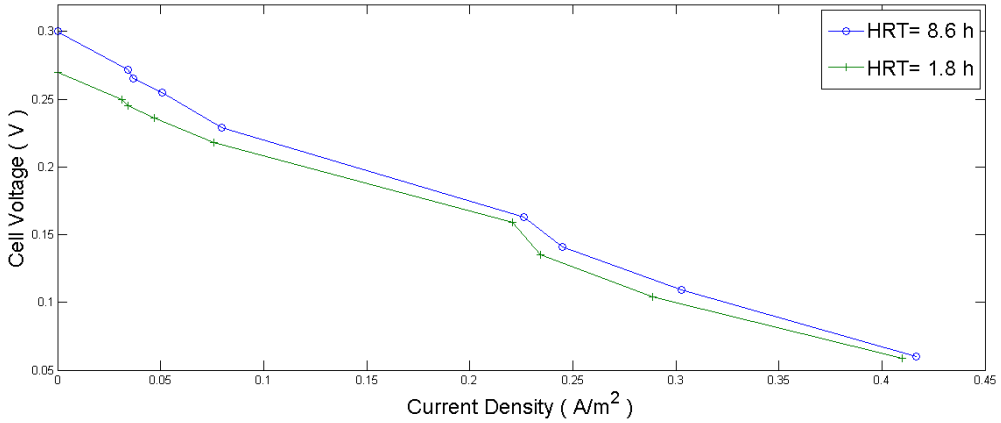


**(b)** Polarization curves: cell voltage vs. current density normalized by cathodes area (72 $cm^2$)

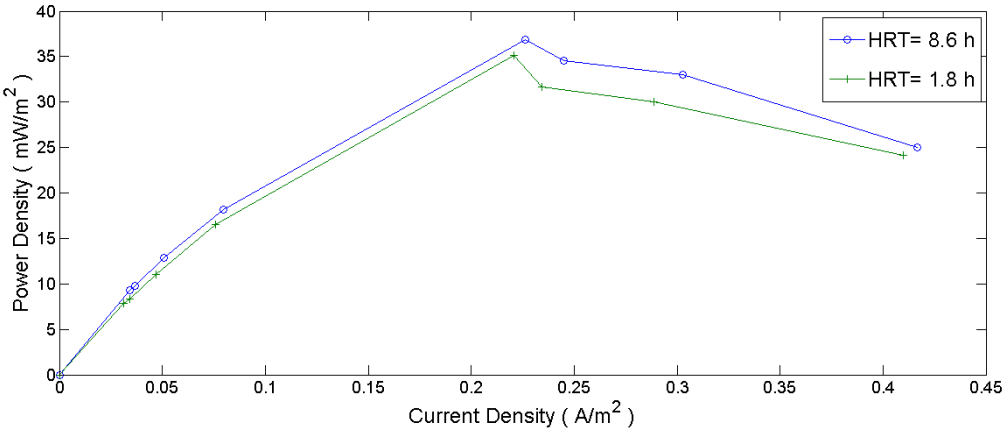


**(c)** Power density curves: power density and current density referred to cathodes area (72 $cm^2$)

**Figure 3.13:** Electrochemical performances comparison at different retention times for the second cell fed with an external organic fuel

affect the cell performances and in all cases the typical voltage trend is observed (Fig.

3.13b and 3.14b): at high resistances from 1110 to 700 Ω the voltage dropped because of the connection at the external load after Open Circuit control (activation loss) and after the ohmic region (linear plot until 100Ω) a more consistent voltage drop is evident but in every test the difference in cell potential at low resistance is not so appreciable. The

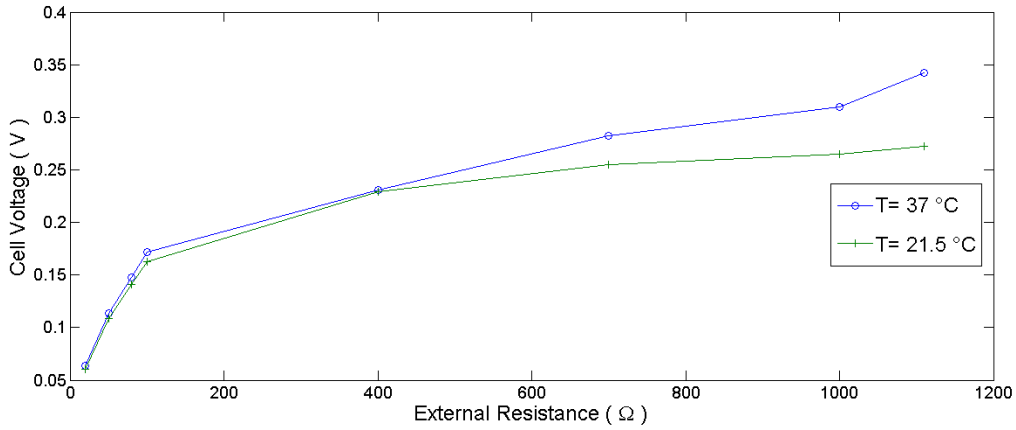


**(a)** Cell voltage recorded by switching external load values

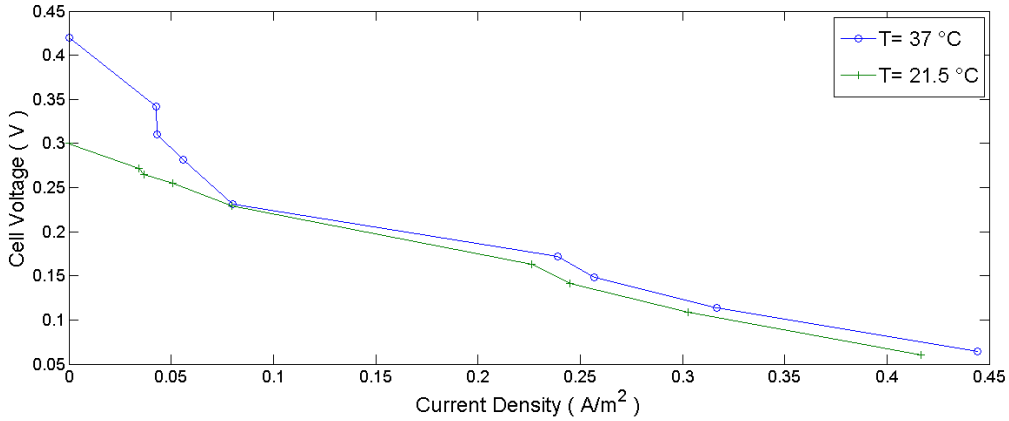


**(b)** Polarization curves: cell voltage vs. current density normalized by cathodes area (72 $cm^2$)

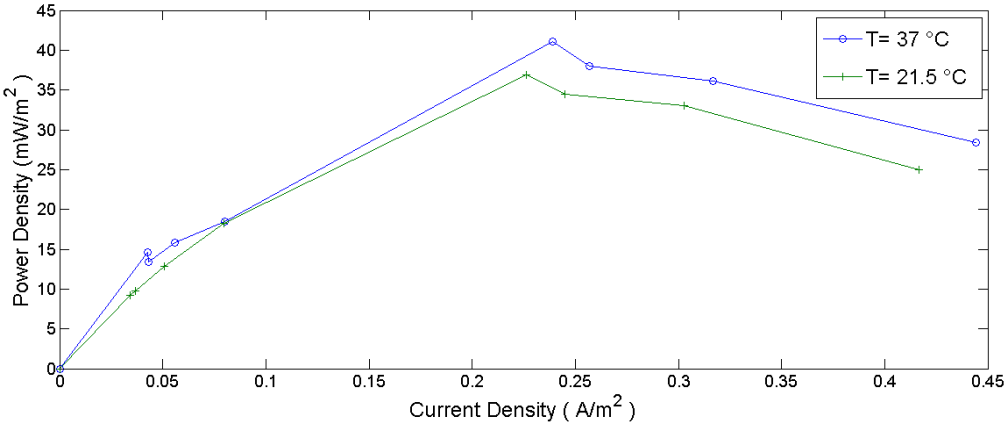


**(c)** Power density curves: power density and current density referred to cathodes area (72 $cm^2$)

**Figure 3.14:** Electrochemical performances comparison at different temperatures for the second cell fed with an external organic fuel

most visible difference is in the temperature comparison (Fig. 3.14b) in which the high

temperature curve shows a higher drop in voltage at low current densities. In this condition the activation losses are more consistent and the cell voltage is not positively affected by the increase of temperature because from 400Ω onwards the voltage values are very similar. The power density curves (Fig. 3.13c and 3.14c) are also important to compare the efficiencies of the cell at different conditions but they show similar trends and close values: very small differences characterise the retention time comparison (Fig. 3.13c) and the higher power density value (41 mW/$m^2$) was reached when the cell was run at high temperature (37 °C) and in this condition a sort of power overshoot can be observed (second and third point of the curve) whose reason can be the higher enzymatic activity at elevated temperature that does not lead to stable and high current generation at low external load with a rapid decrease in power density trend.

### 3.5.2 Current generation over time

Fig. 3.15 and 3.16 are interesting to evaluate the stability of current produced during substrate removal because these are the conditions in which the cell is supposed to work in a real application. For each cell the first sample withdrawn was the one at high retention

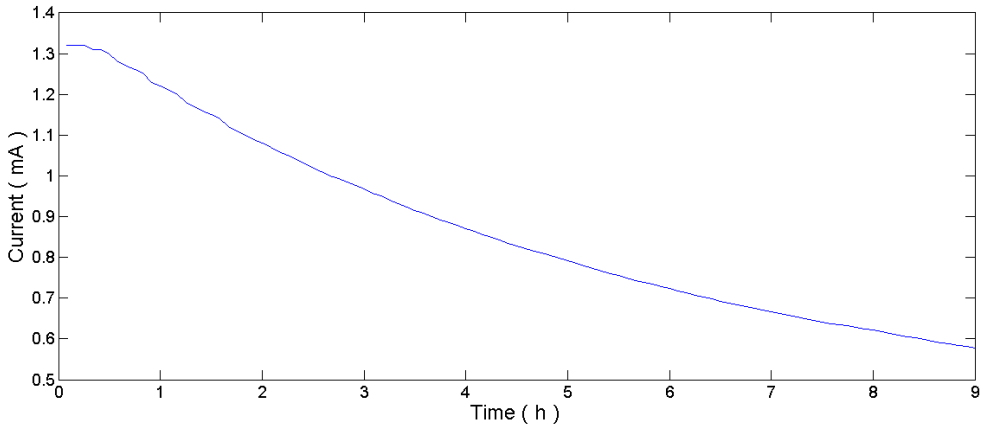


**(a)** Current produced during COD removal at high retention time

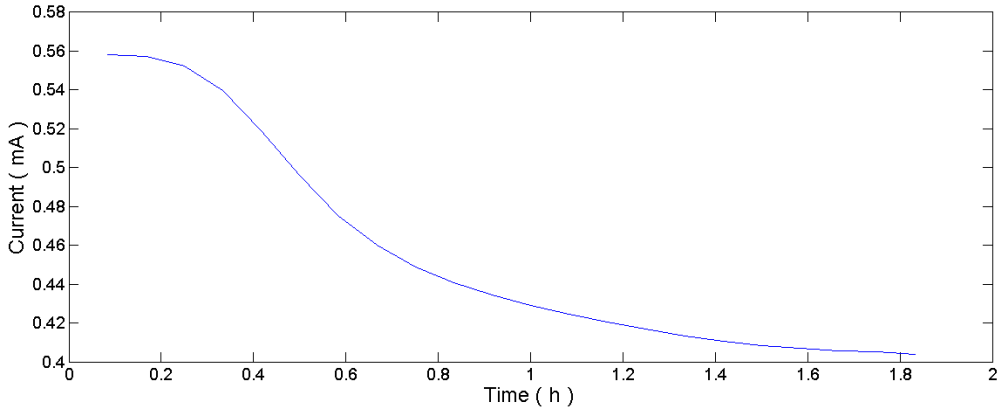


**(b)** Current produced during COD removal at low retention

**Figure 3.15:** Current decay trend for the first cell fed with raw waste water during COD removal

time and afterwards the low retention time was tested: both cells are characterized by a flat trend at the beginning of the experiments (around 20 min) hence a current decay is observed. The first cell went through a slighter decay at both retention times compared to the second cell: 0.05 and 0.08 mA/h are lost respectively at low and high flow rate by the first cell and 0.16 and 0.2 mA/h are the decay rate of the second cell at the same flow rate.

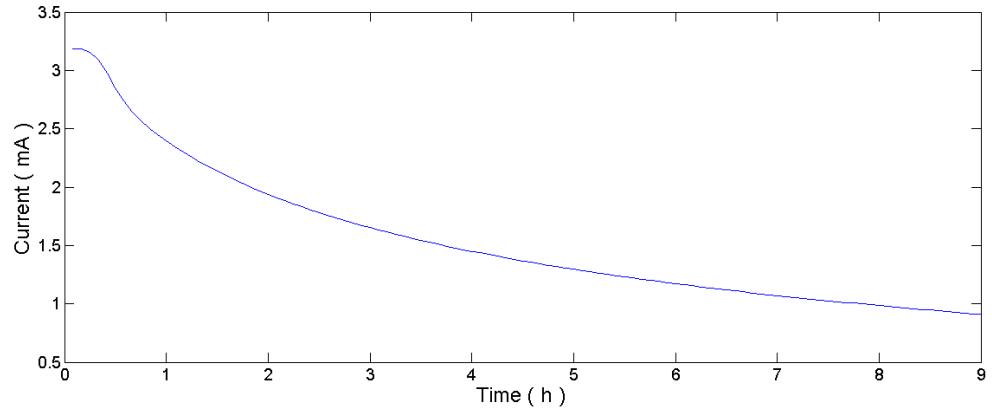


**(a)** Current produced during COD removal at high retention time

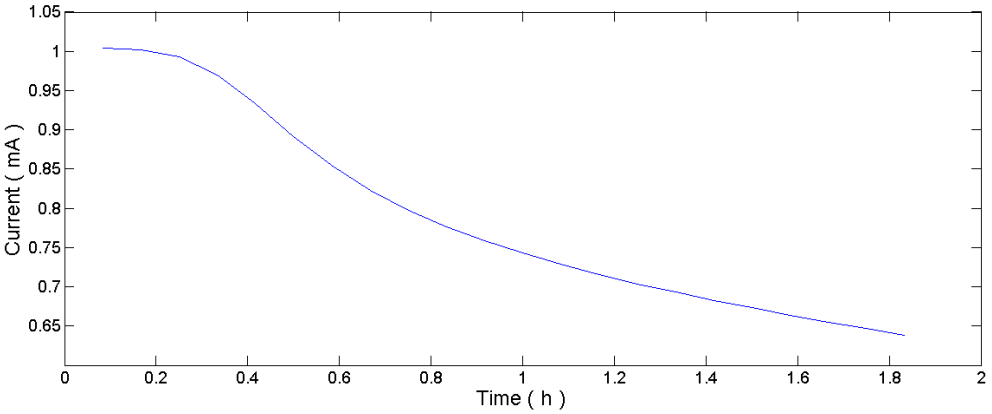


**(b)** Current produced during COD removal at low retention time

**Figure 3.16:** Current decay trend for the second cell fed with raw waste water during COD removal

This values are not significant because of the low currents achieved but they are important to compare the two cells that differed in biofilm age and stability. The lower current decay rate of the first cell can be justified by the greater time of acclimation of the biofilm that could thrive more than the second one.
High flow rate for both cells conduce to higher current decay than low flow rate and it is likely due to disturbances to the biofilm even though the high flow rate should supply more nutrient to the bacteria and enhance the mass transport.
A main factor affecting current generation is solution conductivity: raw waste water was inoculated in the cells to not affect the substrate concentration and hence the analysis results but the lack of the medium solution containing the phosphate buffer involves a lower conductivity in the electrolyte and a lower current as well according to the electrochemical principle that the greater is the ions flux in the electrolyte solution the higher is the electrons flow in the external circuit.

### 3.5.3 Cyclic voltammetry

#### First cell voltammetry

The curves obtained from the two cyclic voltammetry tests of the first cell are shown below. Both of them were produced by the cell run at 21.5 °C and 8.6 h Hydraulic Retention Time.

The typical sigmoidal trend is observed (Fig. 3.17) but it is not detected the flat curve at higher potentials that is present in other studies [14, 22] therefore this result could be

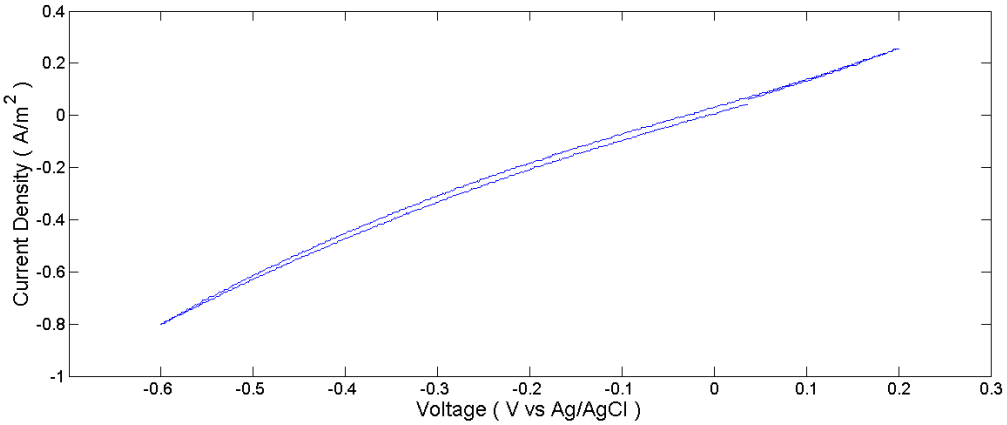


**Figure 3.17:** Cyclic voltammetry of the first cell run at 21.5 °C and 8.6 h HRT at 1 mV/s scanning rate

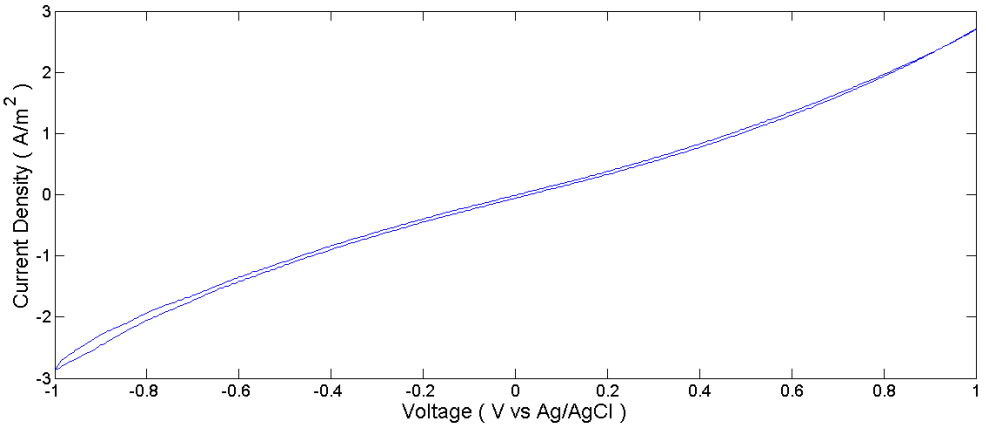


**Figure 3.18:** Cyclic voltammetry of the cell with a wider range of potential at 10 mV/s scanning rate

affected by a high ohmic loss in the capillary in between the cell and the reference electrode which affects the working electrode potentials used to measure the current extracted. The plot obtained show a very high resistance that affects the curve shape.
Even scanning the potential at higher ranges (from -1 V to +1 V vs. reference, 3.18) the sigmoidal shape is observed but the current plateaux is still missing.
Another reason for this different cyclic voltammetry curve could rely on the carbonaceous source used to feed the bacteria: in this case before the test the cell solution (composed by waste water and medium in 1:1 ratio) was amended with 1 g/L of glucose but in the researches cited as reference [14, 22] the only carbon source added to the medium feeding the cell was acetate which is known to favour an higher accumulation of *Geobacter sulfurreducens* that is particularly specialized on acetate.
The cyclic voltammetry scan is an useful method to detect the over-potential vs. current trend which according to Butler-Volmer equation permits to determine the limiting step of the process. A flat curve of potential indicates a mass transfer limitation that is not observed in these plots whose shapes are more likely due to a kinetic limitation. The nutrient contained in the waste water (organic matter and glucose added as extra fuel) can easily reach the biofilm that oxides it on the anode surface and this reactant supply is faster than the oxidation reaction which appears to be limiting. In this case the solution flow rate is the lowest used and the temperature is the room temperature at which the cell was run for over a

month: as the mass transport is not effective on the potential it is probably useless to repeat the test under higher flow rate (low retention time) but it is more interesting to evaluate the effect of temperature on the curve since the enzymatic processes involved in the oxidation reaction are supposed to be faster at high temperature (compatible with microorganism life).

Cyclic voltammetry on the second cell was conduced both on the anode and the cathode electrode to determine the limiting factors of the different reactions on the electrodes.
Both electrodes curves show hysteresis phenomena 3.19 hence the open circuit potential (zero current extracted) is reached at different voltages in the cycle.

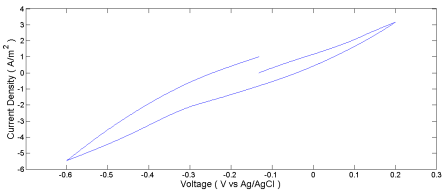


**(a)** Cyclic voltammetry of anode as working electrode with current normalized by anodic area

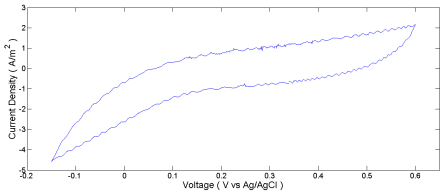


**(b)** Cyclic voltammetry of cathode as working electrode with current normalized by cathodic area

**Figure 3.19:** Cyclic voltammetry of both second cell electrodes at 1 mV/s scan rate

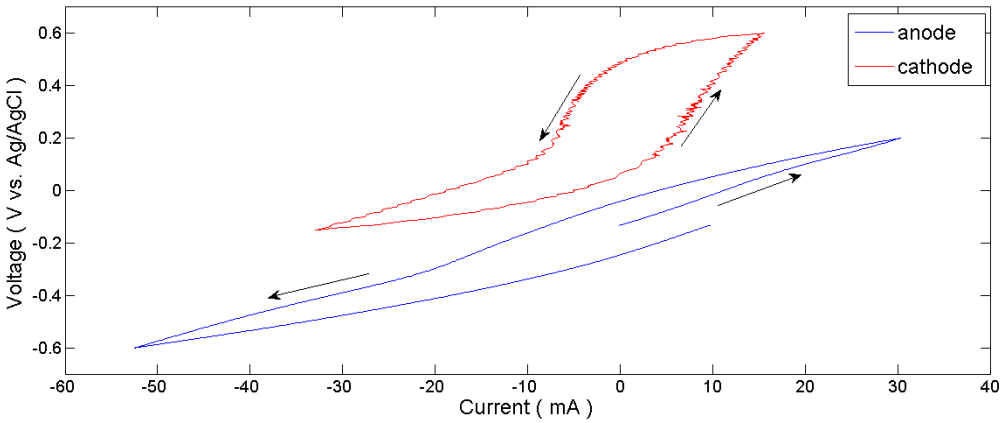


**Figure 3.20:** Cyclic voltammetry of cathode as working electrode at 1 mV/s scan rate on the second cell

The current values were normalized by electrodes area to compare the plots with other researches and the last cycle of every cyclic voltammetry scan was reported: from the anodic curve (Fig. 3.19a) a sigmoidal shape can be observed even though it does not achieve a plateau at high potentials as in other studies [9, 22] but this plot can be compared with the ones deriving from biofilm formed by bacteria contained exclusively in waste water [14] that is the case of this study.
The anodic trend shows the main inflection point of the sigmoidal curve between -0.4 and -0.3 V (vs. Ag/AgCl) that is also observed in cells in which the source for microbial inoculum was primary waste water. The second part of the plot at high potentials (after the inflection point) differs from typical cyclic voltammograms of MFC probably because of the organic compound used to enhance bacteria activity: glucose was added to the waste water and medium solution in this work while sodium acetate is the most utilized electron donor in other researches and it is known that this compound is responsible for the proliferation of *Geobacter sulfurreducens*, an electroactive organism specialized on acetate and that can

cause the plateau of voltammogram.
A completely flat cyclic voltammogram would be obtained if the cell was run without substrate addition (the anode used in the study was also a carbon electrode) [9] but it is not the case hence a mass transport limitation can be excluded.
The scan rate of 1 mV/s appears to be low enough to represent the stationary characteristics of the electrode: from the chronoamperometry test used to stabilize the anode to low potentials a current density of 0.64 A/$m^2$ was recorded and from the cyclic voltammetry at the same potential applied in the chronoamperomety (-0.157 V vs Ag/AgCl) the current density obtained was 0.78 A/$m^2$.
Current density values obtained in the plot are similar to other results obtained with microbial biofilm composed by waste water bacteria [14] (about 50 $\mu A/cm^2$) at low anode potentials.
The cyclic voltammetry test in this case is not indicative of the species present in the biofilm since similar shapes were not detected in other studies but the reason of this differences should rely on the different conditions of the test: the inoculation of acetate with medium solution in the cell conduces to a sigmoidal curve with a plateau at high voltages due to the favourable developing conditions for *Geobacter sulfurreducens* while in this study the carbonaceous source for bacteria was waste water and the glucose amendment that probably induce a different bacteria selection.
Another affecting factor of anode performances is the biofilm potential of inoculation phase: in this study the polarization of the anode was achieved with a chronoamperometry after one week of open circuit control while a longer anode acclimation at lower potentials (from -0.2 to -0.4 V vs Ag/AgCl) resulted in a more active bacteria culture that would be also more stable in generating high currents. In Fig. 3.21 the electrodes voltages are represented

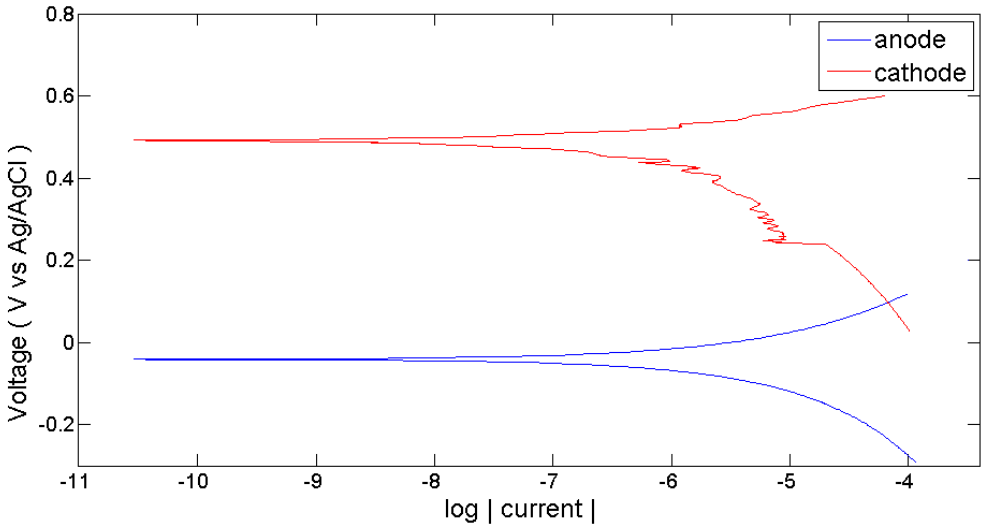


**Figure 3.21:** Logarithmic trend of anode and cathode electrodes vs current produced at 1 mV/s scan rate on the second cell

vs reference electrode depending on current measured during the cyclic voltammetry and the cell voltage is represented by the difference between cathode and anode potential at each current density achieved: the open circuit voltage corresponds to the absence of current (0.55 V) then the cell voltage shrinks with higher currents until a very low voltage at current densities close to 2 A/$m^2$.
In this graph the cathode voltage reaches values close to the thermodynamic reduction potential of oxygen at neutral pH: 0.8 V vs SHE even though the voltage drop at higher current density is evident.

The potential decay shows a very steep slope and that can be due to mass transport limitation: since the cathodic reaction is the oxygen reduction the reactants missing on the electrode surface can be both the ions and electrons produced in the oxidation reaction on the anode and the oxygen diffusing from air. The lack of electrons and protons could be caused by the low efficiency of biofilm in catalysing the substrate oxidation reaction because of the short acclimation and hence the poor stability of exoelectrogens in the biofilm. The oxygen diffusion can be limiting because the air cathodes receive the reagent from the outside but no oxygen flow was provided to replace the reactant consumed in the reaction so only natural convection was involved in oxygen supply and the low concentration in air (21 %) makes this step a possible limiting factor.
The anode electrode was acclimated at low potential with the chronoamperometry technique but the starting value seems to be too high to achieve elevated current density and a longer acclimation at lower potential (other researches showed promising results with anodic biofilm formed at -0.4 V vs SCE [9]) could positively affect the anode performances leading to higher current densities.

## 3.6 Substrate removal

**Table 3.3:** Substrate removal analysis results

| Cell | Retention Time (h) | Resistance (Ω) | COD (mg/L) |
|---|---|---|---|
| Initial value | | | 334 |
| 1 cell | 8.6 | 100 | 550 |
| | 1.8 | 100 | 572 |
| 2 cell | 8.6 | 100 | 441 |
| | 1.8 | 100 | 248 |
| | 1.8 | Open Circuit | 369 |

Between the values obtained in the biological analysis the most surprising are the COD levels because they are higher than the original water (334 mg/L) except for the second one at low retention time and it can be explained by the glucose periodical addition in both cells. The cells were not emptied and refilled with the new solution before sampling to not damage bacteria biofilm but in this way probably the high concentration of glucose affected the measure. This reason can be the most reliable in fact the second cell at high flow rate with external load was the last one tested and the cell was fed with glucose more than two days before hence it was the less affected by this contamination. Though the first cell was the most influenced and it shows the highest COD contents: since the cell was run for almost two months when the samples were taken, the glucose amendment was more relevant.
However from the only test that showed a COD removal (second cell at low retention time) Coulombic Efficiency can be calculated as shown below and the current plots over time recorded during substrate removal are reported in Fig. 3.15 and 3.16.

### 3.6.1 Coulombic Efficiency

Coulombic efficiency of the second cell is calculated from the low retention time sample as it was the one less affected by the glucose addition and showing COD removal: the COD contained in waste water could be in principle all oxidized by exoelectrogens bacteria and the total Coulombs available from the oxidation of $\Delta COD$ corresponds to the denominator in eq. (3.1).

The real Coulombs produced are calculated in the numerator by integrating the current generated during the removal: the area of Fig. 3.16b is obtained as the sum of trapezoids and the time span of integration depends on the retention time of the solution in the cell since it was assumed that during that time the bacteria removed the substrate and at the same time produced energy.

$$C_E = \frac{M_s \quad \int_0^t I\,dt}{F \quad b_{es} \quad \nu_{An} \quad \Delta COD} = \frac{8 \cdot 4.958}{96485.333 \cdot 36 \cdot 86 \cdot 10^{-6}} = 13.3\% \tag{3.1}$$

The value obtained is low compared to other devices tested with raw waste water [21] like in this study but it is still an acceptable value for a upstream device in continuous flow conditions. Oxidizing substrate is hence removed mainly by aerobic and anaerobic bacteria not able to transfer electrons to the electrode surface: the anodic biofilm is not well acclimated and the natural bacteria selection in the microorganism culture was not able to make the exoelectrogens bacteria thrive more than the others.
All the researches focused on substrate removal [10, 21] used an anode electrode acclimated with the effluent solution from a cell run for more than one year and this can be a fundamental factor in exoelectrogenic bacteria selection. The microbial inoculum can also be selected to favour the growth of desired bacteria and a more efficient, electron producing biofilm should be achieved.

### 3.6.2 Nitrification and denitrification

**Table 3.4:** Substrate removal analysis results

| Cell | Retention Time (h) | Load (Ω) | Total N (mg/L) | Removal % | Removal rate (kg $m^{-3}d^{-1}$) |
|---|---|---|---|---|---|
| Initial value | | | 54 | | |
| 1 cell | 8.6 | 100 | 15 | 72.2 | 0.109 |
| | 1.8 | 100 | 36 | 33.3 | 0.24 |
| 2 cell | 8.6 | 100 | 50 | 7.4 | 0.011 |
| | 1.8 | 100 | 45 | 16.7 | 0.12 |
| | 1.8 | Open Circuit | 44 | 18.5 | 0.133 |

Nitrogen contents in the effluents are interesting for the trend shown and for the specific values that represent a discrete substrate removal.
In Tab. 3.4 the removal efficiency of the two cells are presented: the total nitrogen content is lower for the test conduced at high retention time in the first hence this condition assures also a higher percent removal.
The final value obtained can be due to the long period of work of the cell that could develop a well acclimated biofilm containing nitrifying and denitrifying bacteria.
The second cell produced different results that are however coherent with the explanation given above for the first cell: the last cell was tested after two weeks from the start-up and a well structured biofilm was probably not formed. The differences between two retention times used are very small (Tab. 3.4) and therefore the bacteria efficiency could be the limiting factor instead of operational conditions.
From the same set of data nitrogen removal rate is calculated considering the retention time as the time of removal and a comparison of the two devices can be represented: the first cell achieved better results and the higher flow rate conduced to higher removal rate. Total nitrogen values are important to evaluate the possible application of this technology in a real waste water treatment plant: the most common process train includes a denitrification

unit followed by the nitrification step.
Nitrification is limited by low levels of $O_2$ while denitrification requires low dissolved oxygen: levels between 1.97 and 4.35 mg/L do not significantly affect denitrification and are favourable for nitrification [18]. In this study an oxygen detection was not carried out but it would have been useful and only the total nitrogen present is used to estimate the cell efficiency in substrate removal.
Oxygen consumed in nitrification is negatively effecting for the current generation since the reactant of cathodic reaction of oxygen reduction is depleted even though protons produced in nitrifier biofilm can react with diffusing oxygen on the cathode, lowering the charge transfer resistance of the system [19].
In normal sewage processes the optimal COD:N ratio is above 7 but for Microbial Fuel Cell an initial ratio between 4.35 and 5 is acceptable. The water tested in this work the initial COD and nitrogen values of 334 mg/L and 54 mg/L respectively conduced to a ratio of 6.2 which is close to the optimal value and the removal processes are theoretically promoted.
Nitrogen removal rate of both cells are promising for future applications if compared to previous works [18] in which rate of 0.104 kg $m^{-3}d^{-1}$ is reached while in this work the first cell showed the highest rate at high flow rate (0.24 kg $m^{-3}d^{-1}$) and a lower but also relatively high rate at greater retention time (0.109 kg $m^{-3}d^{-1}$).
The second cell with a younger and acclimated biofilm reached lower values (0.12 and 0.01 kg $m^{-3}d^{-1}$ respectively at high and low flow rate).
Total nitrogen content in the water is the sum of several nitrogen compounds that take part in different reactions and can be consumed by the microorganisms:

$$TN = [Organic \quad N] + \left[NH_4^- - N\right] \left[NO_2^- - N\right] + \left[NO_3^- - N\right] \tag{3.2}$$

The feeding solution contains a small amount of nitrite and nitrate (0.02 and 0.33 mg/L-N) and the ammonia component is the most relevant since the initial concentration was 46.9 mg/L-N.
The total nitrogen removal in the cells can be due to nitrification and denitrification reactions on the cathode surface and in the anodic solution: nitrogen bound to organic compounds was not examined in the effluent solution but it was probably removed at least in a small percentage since the lowest value of final total nitrogen achieved is 15 mg/l (first cell high retention time) and the organic nitrogen at the beginning was 6.75 mg/L-N hence if organic nitrogen was not removed, all the nitrogen removal can be adduced to ammonia consumption (nitrate and nitrite are in small quantities) and the specific ammonia removal would be 70% of the initial value which is lower than other works [19] although these devices are not old enough to be compared with other cells.
Ammonia loss through air cathodes was observed in previous researches and it can affect the final amount of nitrogen detected in the samples but even if this loss was not analysed directly it seems that the diffusion layer (0.7 mm thickness) can greatly reduce this loss and the difference in nitrogen content between the two cells can confirm this hypothesis: they have the same diffusion layer composition (Teflon-based) and thickness but the first cell reached higher removal most likely because of the longer running period in which the biofilm could enrich in nitrifying and denitrifying bacteria.
In order to enhance nitrification it has been proposed [19] to enrich the cathode biofilm with nitrifying bacteria since they can suffer from competition with heterotrophs and show a lower growth in a mixed culture leading also to an improvement in power densities generated.
Nitrifying bacteria need oxygen to catalyse the oxidation reaction and in a mixed culture as a sewage microbial inoculum, they thrive close to the cathode electrode where the higher oxygen concentration is reached in the cell.
Denitrifying bacteria have more complex proliferation pathways: they should be predominantly enriched in the anode suspension rather than on the electrode surface [4] and receive

electrons from substrate oxidation but they can also colonize the cathode biofilm and catalyse the reduction reaction of denitrification with electrons flowing from the anode.
In other researches [19] the study of the cathodic biofilm permitted to suppose that the organic substrate utilization as electron donor was predominant in the early stage of operation and during a longer phase operation denitrifiers may compete with nitrifiers in colonizing the cathode surface according to their tolerance to oxygen concentration.

### 3.6.3 pH evolution

An indirect analysis of reactions occurring in the system can be done looking at the pH levels in the effluents (Tab. 3.5): the little change in pH (initial value was 7.23) is consistent with other works [19].
Nitrification reactions (eq. 3.3 and 3.4) involve protons production and a pH drop although the reduction reaction of denitrification (eq. 3.5) might partially offset the pH change if the denitrifiers are settled in the cathode biofilm.

**Table 3.5:** Substrate removal analysis results

| Cell | Retention Time (h) | Resistance (Ω) | pH |
|---|---|---|---|
| Initial value | | | 7.23 |
| 1 cell | 8.6 | 100 | 7.4 |
| | 1.8 | 100 | 7.14 |
| 2 cell | 8.6 | 100 | 7.34 |
| | 1.8 | 100 | 7.54 |
| | 1.8 | Open Circuit | 7.18 |

$$NH_4^+ + 2H_2O \longrightarrow NO_2^- + 6e^- + 8H^+ \tag{3.3}$$

$$NO_2^- + H_2O \longrightarrow NO_3^- + 2e^- + 2H^+ \tag{3.4}$$

$$NO_3^- + 5e^- + 6H^+ \longrightarrow 1/2N_2 + 3H_2O \tag{3.5}$$

Oxygen reduction at the cathode is also a protons consuming reaction but it is coupled with the oxidation reaction of substrate on the anode that produces an equivalent amount of protons which react on the cathode after flowing through the solution thereby a good ions conductivity would make the pH in the bulk solution almost unchanged.

$$O_2 + 4H^+ + 4e^- \rightarrow 2H_2O \tag{3.6}$$

## 3.7 Corrosion phenomena

The cathodes used in the first cell made by nickel mesh showed some corrosion effects on the air-side surface and the green spots visible on it (Fig. 3.22a) can be due to nickel oxide deposition meaning that secondary reactions could affect the cathodic reaction of oxygen reduction. The white crystals present on the grid (Fig. 3.22b) can be the effect of salt deposition since the medium solution inoculated into the cell to enhance the conductivity contains a significant amount of salts.
The white crystals are mainly observed on the cathode which is on the reference electrode side and to better understand the type of crystals further analysis would be necessary since no difference in solution characterizes the two electrodes except for the capillary in between the anode and the cathode with the bigger salt depositions.

**(a)** Cathode electrode with nickel deposition.

**(b)** Cathode electrode with green spots and salt crystals.

**Figure 3.22:** Corrosion effects on the cathode electrode: green spots on both sides. Salt deposition with white crystals mainly on the side of reference electrode

# Chapter 4

# Conclusions

## 4.1 Electrodes performances

### 4.1.1 Anode electrode

The vitreous carbon foam used as anode electrode can be considered a good material for biofilm growth thanks to the high porosity (96.5 %) and the relatively small pores size (below 3000$\mathring{A}$).
The main drawback of the anode configuration was the connection with the external circuit: the titanium wire tightened around it did not assure a good electrical connection and increased the electrode resistance affecting the total cell performance.
In latest studies on Microbial Fuel Cells a brush anode is used with carbon fibers as electrode material and two titanium wires twisted around them working as current collector: this configuration is rather advanced for the high conductivity of the electrode (carbon fibers have lower internal resistance than vitreous carbon), for the high ratio surface:volume due to the small thickness and the high number of the fibers and for the good connection with the current collector: in this project the titanium wire did not show a good contact with the foam for all its length and this conduced to a lower conductivity of the entire electrode.

### 4.1.2 Cathode electrode

The air-cathode electrode working in the first cell showed good efficiency in preventing water leakage but because of the reference electrode low reliability no voltammetry test was conduced on the electrode hence no electrochemical feature can be compared with the others produced for the second cell.
Corrosion phenomena were observed on the nickel mesh surface and decrease in cathode voltage could be caused by mixed potential on the electrode surface deriving from the overlap of oxygen reduction reaction and nickel dissolution.
Salts deposition can also be detected on electrode surface (white crystals were clearly observed after more than one month of operations) coming from the solution containing both salts in the waste water and in the buffer solution. Although the separator put on the cathode surface should diminish cathode biofouling.

The cathodes realized for the second cell were tested for a shorter time thereby no salt deposition was observed. However the stainless steel mesh is a corrosion resistant material and AISI 316 is one of the most suitable material for environments with corrosion risk.
The low price of stainless steel and the good electrical connection provided by the grid piece coming out from the cell make this material preferable to nickel electrodes.
The diffusion layer on the cathode surface was equal to the previous one hence no water leakage was recorded in the operation period and the better reference configuration allowed

to conduce electrochemical analysis on the electrode.
After two weeks of operations the cathode potential was 0.68 V vs SHE and it can be consider quite promising since the thermodynamic reduction potential of oxygen is 0.805 V vs SHE. This result induce to think that the platinum is still one of the most performing catalyst for this reaction and the only disadvantage for real applications is the high price.

Possible future developments of this device should take into account the possibility of manufacturing a greatly cost-effective cathode with high catalytic properties. In that sense, the cathodes realised for the second cell and failing the leakage test seem to be a promising alternative to platinum based electrode: the idea of a single layer containing either the catalyst and the hydrophobic compound for leakage prevention can lead to easier production procedures and the phase inversion step mentioned in the paper followed for the realization, could be very cost-effective compared to traditional methods in which thermal and mechanical treatment are needed to dispose of the solvent.
The very challenging point of this technique is the catalyst used: activated carbon is either a cheap and efficient material but the long term reliability of this compound has not been tested yet. It is also true that the purpose of the author was to use the catalyst in the gas phase reaction where oxygen has higher concentration hence probably the lower catalytic properties of activated carbon compared to platinum can be balanced by enhancements in kinetic control of the reduction reaction.
The recipe followed for the electrodes realization is still very promising but different ratios of reactants should be tried and especially the binder amount (PVDF) in order to avoid cracks in the phase inversion reaction: if necessary another way of removing the solvent should be discovered and tested because electrodes as big as the ones utilized in this work proved that this procedure is not suitable with such dimensions.

## 4.2 Start-up phase

Biofilm formation is one of the most important and characteristic step in MFc operations: both cells showed a 3 days lag time for voltage increase due to bacteria activity. During this period the microorganisms colonized the electrode and gather together to form a well structured biofilm, after the lag period biofilm started producing electrons and the cell voltage increased.
First cell biofilm was naturally acclimated and no external input was given to the electrode and the biofilm while the second cell anode was slightly polarized after one week and that increased total cell voltage because a lower anode potential (0.04 V vs SHE) positively affects the biofilm activity and its electrons transfer and subsequently the counter reaction (oxygen reduction) is enhanced on the cathode surface leading to higher cathodic potentials. For this reason a longer polarization phase looks beneficial for biofilm activity: bacteria acclimated at low potentials (lowest voltage applied in other studies is -0.4 V vs. Ag/AgCl) are more efficient and stable releasing more electrons and increasing total current generation. In this sense a stainless steel electrode based as the cathodes used in this work (AISI 316) can be the right choice for the high resistance to corrosion and polarization tests can be conduced without risk of damaging the electrode: first cell cathodes were not properly corrosion resistant because of the nickel mesh support and nickel oxide deposition were evident after a relative long operational period (one month).

## 4.3 Electrochemical performances

Both cells reached low power productions and this result is likely due to the short acclimation time of the systems: 0.23 mW and 0.3 mW are the maximum powers generated

by respectively, the first and the second cell. Power density greatest values are thereby 32 mW/$m^2$ and 41 mW/$m^2$ for the first and the second system referring to cathode surface (72 $cm^2$). These results can be compared to other works that generally achieved higher values of power density (10 times higher) but several differences could affect this comparison: the cells operated in this study were acclimated for less the two months (first cell) and two weeks (second cell) while it is common to run the cell for more than one year and then insert the anode with the biofilm grown on it in a new cell and test the system with the buffer solution and the organic fuel (generally acetate) addition.
The devices designed and tested in this study were not mature enough to produce a significant current and electrical power and probably a longer time of operation would be beneficial for the electrochemical efficiency. A selected bacteria culture could also favour the biofilm formation since the anaerobic environment supports the exoelectrogens development but it would be more directly effective to inoculate the cell with a selected exoelectrogenic bacteria culture shortening the start up phase and improving the power production.
In order to enhance the current generation, the cells should be run with a high conductivity solution but in this case a 1:1 ratio between waste water and buffer solution was used for both cells because the not well acclimated biofilm needed bacteria inoculation for all the operational period. A higher conductivity greatly affects current generation since the electrons flow in the external circuit has to be balanced by ions flux in the electrolyte.
Another important difference is devices sizes: the cells built in this work are bigger than other laboratory scale fuel cell. For this reason current and power normalized by cathode geometrical area are lower compared to other researches in which the electrodes dimensions are much smaller. To obtain a higher performances all the resistances in the system should be decreased: the anodic connection is not very efficient because of the titanium wire tighten up around the foam and the electrolyte resistance is probably too high for the low conductivity due to waste water.
Different parameters effects were analysed in both cells and it seems that neither the temperature or the retention time are very effective on the cells performance: temperature has more influence at high voltage (low external resistance) because of the enhancement of bacteria activity at elevated temperature but the drop in voltage due to ohmic losses is similar to other conditions hence for power production this parameter is not very determining. Different flow rate conditions lead to polarization and power density curves almost similar thereby this parameter can be considered a fundamental parameter only for substrate removal and not for electrochemical performances.
Although these results are mainly influenced by the biofilm poor activity due to the short acclimation period: the cell potential showed a substantial decrease when the external load was applied hence a polarization effect was noticed in the system and meaning that the bacteria were not able to produce the same amount of electrons requested by the external circuit. In all experiments the first test was the most efficient then the decrease in cell potential conduced to lower electrochemical efficiency.

The importance of biofilm stability is appreciable in the current drop during substrate removal: first cell decreased current produced from 1.32 to 0.37 mA while second cell showed a higher starting value (3.2 mA) but a greater decrease with a final current of 0.6 mA and hence a higher drop likely due to lower acclimation of the second cell exoelectrogens microorganisms.

## 4.4 Substrate removal

Nitrogen removal was the most important result achieved by the systems during biological analysis: 72.2% of total nitrogen removal was obtained by the fist cell at the lowest flow

rate and the difference in removal efficiency between the two devices (maximum removal of the second cell was 18.5%) tested can be explained with the longer operational period of the first cell. Nitrifying and denitrifying bacteria had to thrive in a mixed culture and a longer time of growth is beneficial for them: nitifying bacteria have to reach the cathode side and colonize it in order to consume oxygen flowing from the net in the nitrification reaction, denitrifying bacteria firstly operate in the anodic solution carrying out the reduction reaction with the electrodes produced in the substrate oxidation, then they are supposed to mix with the nitrifying bacteria on the cathode and use as electron donor the electrode itself which receives electrons from the external circuit.
Even if these results look promising for the real application of MFC in waste water treatment the enrichment of cathode biofilm with nitrifying bacteria has been proved to enhance the substrate removal hence as for the exoelectrogenic anodic biofilm, the selection of specified bacteria would be positive for the system and improve nutrient consumption as well.
COD values were affected by the high amount of glucose added during the start up phase of both cells and only the second system reached an appreciable substrate removal which let calculate the coulombic efficiency of the cell but the low value (13.3 %) induces to conclude that the exoelectrogenic bacteria were not well developed and a longer time of acclimation or a specific inoculation with these microorganisms would have been necessary.
Values of pH in the effluents are almost similar to the initial sewage and that can be due to the offset in protons production and consumption between nitrification and denitrification reactions while the organic matter oxidation provides ions to the counter reaction on the cathode and they should be in the same amount in a well buffered system.

# Bibliography


[1] Peter Clauwaert, Korneel Rabaey, Peter Aelterman, Liesje De Schamphelaire, The Hai Pham, Pascal Boeckx, Nico Boon, and Willy Verstraete. Biological denitrification in microbial fuel cells. *Environmental Science & Technology*, 41(9):3354–3360, 2007.

[2] Yue Dong, Youpeng Qu, Weihua He, Yue Du, Jia Liu, Xiaoyu Han, and Yujie Feng. A 90-liter stackable baffled microbial fuel cell for brewery wastewater treatment based on energy self-sufficient mode. *Bioresource technology*, 195:66–72, 2015.

[3] Benjamin Erable, Narcis Duteanu, SM Senthil Kumar, Yujie Feng, Makarand M Ghangrekar, and Keith Scott. Nitric acid activation of graphite granules to increase the performance of the non-catalyzed oxygen reduction reaction (orr) for mfc applications. *Electrochemistry Communications*, 11(7):1547–1549, 2009.

[4] Chunhua Feng, Liqiao Huang, Hui Yu, Xiaoyun Yi, and Chaohai Wei. Simultaneous phenol removal, nitrification and denitrification using microbial fuel cell technology. *Water research*, 76:160–170, 2015.

[5] Yiying Hong, Douglas F Call, Craig M Werner, and Bruce E Logan. Adaptation to high current using low external resistances eliminates power overshoot in microbial fuel cells. *Biosensors and Bioelectronics*, 28(1):71–76, 2011.

[6] Adam J Hutchinson, Justin C Tokash, and Bruce E Logan. Analysis of carbon fiber brush loading in anodes on startup and performance of microbial fuel cells. *Journal of Power Sources*, 196(22):9213–9219, 2011.

[7] Ioannis Ieropoulos, Jonathan Winfield, and John Greenman. Effects of flow-rate, inoculum and time on the internal resistance of microbial fuel cells. *Bioresource technology*, 101(10):3520–3525, 2010.

[8] YU Jin et al. Reaction mechanism on anode filled with activated carbon in microbial fuel cell. *Journal of Chemical and Pharmaceutical Research*, 6(5):333–339, 2014.

[9] Stephanie F Ketep, Alain Bergel, Marie Bertrand, Wafa Achouak, and Eric Fourest. Lowering the applied potential during successive scratching/re-inoculation improves the performance of microbial anodes for microbial fuel cells. *Bioresource technology*, 127:448–455, 2013.

[10] Kyoung-Yeol Kim, Wulin Yang, and Bruce E Logan. Impact of electrode configurations on retention time and domestic wastewater treatment efficiency using microbial fuel cells. *Water research*, 80:41–46, 2015.

[11] Yohannes Kiros. Metal porphyrins for oxygen reduction in pemfc. *Int. J. Electrochem. Sci*, 2:285–300, 2007.

[12] Bruce E Logan. *Microbial fuel cells*. John Wiley & Sons, 2008.

[13] Bruce E Logan, Maxwell J Wallack, Kyoung-Yeol Kim, Weihua He, Yujie Feng, and Pascal E Saikaly. Assessment of microbial fuel cell configurations and power densities. *Environmental Science & Technology Letters*, 2(8):206–214, 2015.

[14] Sunil A Patil, Falk Harnisch, Balasaheb Kapadnis, and Uwe Schröder. Electroactive mixed culture biofilms in microbial bioelectrochemical systems: the role of temperature for biofilm formation and performance. *Biosensors and Bioelectronics*, 26(2):803–808, 2010.

[15] Chikashi Sato, Reymer G Martinez, Malcolm S Shields, Alba Perez-Gracia, and Marco P Schoen. Behaviour of microbial fuel cell in a start-up phase. *International Journal of Environmental Engineering*, 1(1):36–51, 2009.

[16] Supramaniam Srinivasan. *Fuel cells: from fundamentals to applications*. Springer Science & Business media, 2006.

[17] Daniele Vigolo, Talal T Al-Housseiny, Yi Shen, Fiyinfoluwa O Akinlawon, Saif T Al-Housseiny, Ronald K Hobson, Amaresh Sahu, Katherine I Bedkowski, Thomas J DiChristina, and Howard A Stone. Flow dependent performance of microfluidic microbial fuel cells. *Physical Chemistry Chemical Physics*, 16(24):12535–12543, 2014.

[18] Bernardino Virdis, Korneel Rabaey, René A Rozendal, Zhiguo Yuan, and Jürg Keller. Simultaneous nitrification, denitrification and carbon removal in microbial fuel cells. *Water Research*, 44(9):2970–2980, 2010.

[19] Hengjing Yan, Tomonori Saito, and John M Regan. Nitrogen removal in a single-chamber microbial fuel cell with nitrifying biofilm enriched at the air cathode. *water research*, 46(7):2215–2224, 2012.

[20] Wulin Yang, Weihua He, Fang Zhang, Michael A Hickner, and Bruce E Logan. Single-step fabrication using a phase inversion method of poly (vinylidene fluoride)(pvdf) activated carbon air cathodes for microbial fuel cells. *Environmental Science & Technology Letters*, 1(10):416–420, 2014.

[21] Xiaoyuan Zhang, Weihua He, Lijiao Ren, Jennifer Stager, Patrick J Evans, and Bruce E Logan. Cod removal characteristics in air-cathode microbial fuel cells. *Bioresource technology*, 176:23–31, 2015.

[22] Xiaoyuan Zhang, Peng Liang, Juan Shi, Jincheng Wei, and Xia Huang. Using a glass fiber separator in a single-chamber air-cathode microbial fuel cell shortens start-up time and improves anode performance at ambient and mesophilic temperatures. *Bioresource technology*, 130:529–535, 2013.

# Appendix A

# Appendix

## A.1 Acidic activation

The quantities of reactants used for the acidic treatment of the vitreous carbon are showed below. A 65 % solution of $HNO_3$ was diluted with milli-Q water to obtain a 5 % solution. The amount of Nitric acid necessary (mL) was calculated assuming that the final solution volume is mainly due to water, so for a total volume of $V_2 = 600$ mL the solution weight is $m_2 = 600$ g because water density is 1 g/mL.

$$0.65 \cdot m_1 = 0.05 \cdot m_2 \tag{A.1}$$

$$m_1 = \frac{0.05 \cdot 600}{0.65} = 46.15 \quad g \tag{A.2}$$

At this point the acid volume is obtained from $HNO_3$ density $\rho_1 = 1.39$ g/mL.

$$V_1 = \frac{m_1}{\rho_1} = \frac{46.15}{1.39} = 33.2 \quad mL \tag{A.3}$$

The milli-Q water volume necessary to dilute the acid is easily calculated as the the difference between the final volume and the acid volume.

$$V_{H_2O} = V_2 - V_1 = 600 - 33.2 = 566.8 \quad mL \tag{A.4}$$

## A.2 BET Analysis

Data from Brunauer-Emmett-Teller analysis carried on to evaluate the anode surface area are reported below. After a desorption phase in which the sample is heated and a vacuum environment force it to get rid of the gas on its surface, the instrument sends a $N_2$ gas flow to the surface of the material (that is closed inside a tube kept into a bath of liquid Nitrogen) to measure the amount of gas adsorbed which is proportional to the surface of absorption. The second measurement made by the instrument is the pore size and pore distribution investigations that adopt the Barrett-Joyner-Halenda method. From the same set of data it can estimate the average pore diameter and the pore area then the total (cumulative) pore surface area.

## A.3 Cathode Preparation

Since the procedure followed to produce this electrode suggests to use a 10 % PVDF solution (w/v), 3 g of PVDF (Sigma-Aldrich) were dissolved into 30 mL of dimethylacetamide

**Table A.1:** BET Analysis log

| Relative Pressure | Pressure (mmHg) | Volume Adsorbed ($cm^3/g$ STP) | Elapsed time (h:min) | Saturation Pressure (mmHg) |
|---|---|---|---|---|
| | | | 1.42 | 759.8513 |
| 0.011388 | 8.65332 | 0.2626 | 1.52 | 759.8513 |
| 0.03462 | 26.30809 | 0.3816 | 1.54 | 759.8513 |
| 0.069188 | 52.5764 | 0.4548 | 1.57 | 759.8513 |
| 0.080233 | 60.97113 | 0.4797 | 2.00 | 759.8513 |
| 0.100258 | 76.18903 | 0.5194 | 2.02 | 759.8513 |
| 0.120282 | 91.40694 | 0.5442 | 2.04 | 759.8513 |
| 0.140312 | 106.6298 | 0.5626 | 2.06 | 759.8513 |
| 0.160328 | 121.8428 | 0.5483 | 2.09 | 759.8513 |
| 0.199852 | 151.8807 | 0.5522 | 2.11 | 759.8513 |
| 0.219762 | 167.0141 | 0.5727 | 2.13 | 759.8513 |
| 0.26974 | 204.9992 | 0.554 | 2.16 | 759.8513 |
| 0.319711 | 242.9794 | 0.5407 | 2.18 | 759.8513 |
| 0.369649 | 280.9346 | 0.5095 | 2.20 | 759.8513 |
| 0.419636 | 318.9297 | 0.4605 | 2.23 | 759.8513 |
| 0.469427 | 356.7756 | 0.4321 | 2.25 | 759.8513 |
| 0.519413 | 394.7706 | 0.3997 | 2.27 | 759.8513 |
| 0.569268 | 432.6662 | 0.4081 | 2.29 | 759.8513 |
| 0.619187 | 470.6115 | 0.3829 | 2.31 | 759.8513 |
| 0.669101 | 508.5568 | 0.4028 | 2.34 | 759.8513 |
| 0.719018 | 546.5021 | 0.4403 | 2.36 | 759.8513 |
| 0.76875 | 584.3082 | 0.5684 | 2.38 | 759.8513 |
| 0.799938 | 608.0204 | 0.7019 | 2.40 | 759.8513 |
| 0.819986 | 623.2681 | 0.8089 | 2.43 | 759.8513 |
| 0.849773 | 645.916 | 1.0476 | 2.45 | 759.8513 |
| 0.874953 | 665.0626 | 1.2753 | 2.47 | 759.8513 |
| 0.89978 | 683.9408 | 1.5601 | 2.49 | 759.8513 |
| 0.924658 | 702.8588 | 2.0035 | 2.51 | 759.8513 |
| 0.949708 | 721.9108 | 2.6583 | 2.54 | 759.8513 |
| 0.961723 | 731.0517 | 3.2251 | 2.56 | 759.8513 |
| 0.975111 | 741.2368 | 3.8885 | 2.58 | 759.8513 |
| 0.979171 | 744.335 | 4.5519 | 3.01 | 759.8513 |
| 0.990021 | 752.5905 | 5.3669 | 3.03 | 759.8513 |
| 0.994192 | 755.7734 | 17.8289 | 3.06 | 759.8513 |
| 0.994378 | 755.9225 | 31.7046 | 3.08 | 759.8513 |
| 0.99476 | 756.2208 | 46.4472 | 3.10 | 759.8513 |
| 0.995016 | 756.4597 | 60.3335 | 3.21 | 759.8513 |
| 0.995356 | 756.7581 | 75.1817 | 3.31 | 759.8513 |
| 0.995282 | 756.7133 | 62.5725 | 3.34 | 759.8513 |
| 0.995016 | 756.5194 | 48.5499 | 3.36 | 759.8513 |
| 0.994745 | 756.3253 | 33.0622 | 3.39 | 759.8513 |
| 0.988384 | 751.4965 | 11.1245 | 3.41 | 759.8513 |
| 0.956842 | 727.5258 | 10.5029 | 3.44 | 759.8513 |

(DMAc). The PVDF density ($\rho_1$) is 1.74 g/mL and the DMAc density ($\rho_2$) is 0.94 g/mL so

**Table A.2:** BET Analysis log

| Relative Pressure | Pressure (mmHg) | Volume Adsorbed ($cm^3/g$ STP) | Elapsed time (h:min) | Saturation Pressure (mmHg) |
|---|---|---|---|---|
| | | | 3.46 | 760.3486 |
| 0.933416 | 709.7217 | 8.8347 | 3.50 | 760.3486 |
| 0.929426 | 706.6881 | 7.874 | 3.53 | 760.3486 |
| 0.918896 | 698.6813 | 6.2471 | 3.57 | 760.3486 |
| 0.911309 | 692.9125 | 5.0514 | 4.00 | 760.3486 |
| 0.899019 | 683.5679 | 3.9969 | 4.03 | 760.3486 |
| 0.87334 | 664.0431 | 2.7775 | 4.07 | 760.3486 |
| 0.852443 | 648.1538 | 2.0783 | 4.10 | 760.3486 |
| 0.832173 | 632.7419 | 1.5868 | 4.12 | 760.3486 |
| 0.806855 | 613.4908 | 1.2796 | 4.15 | 760.3486 |
| 0.781693 | 594.3591 | 1.0433 | 4.17 | 760.3486 |
| 0.75016 | 570.3834 | 0.8891 | 4.19 | 760.3486 |
| 0.681536 | 518.2048 | 0.6989 | 4.22 | 760.3486 |
| 0.631173 | 479.9114 | 0.6796 | 4.24 | 760.3486 |
| 0.581137 | 441.8665 | 0.6801 | 4.26 | 760.3486 |
| 0.531055 | 403.7869 | 0.6695 | 4.29 | 760.3486 |
| 0.480934 | 365.6775 | 0.7245 | 4.31 | 760.3486 |
| 0.430957 | 327.6775 | 0.7493 | 4.33 | 760.3486 |
| 0.380862 | 289.588 | 0.7696 | 4.36 | 760.3486 |
| 0.330761 | 251.4934 | 0.8348 | 4.38 | 760.3486 |
| 0.28079 | 213.4984 | 0.8403 | 4.40 | 760.3486 |
| 0.230754 | 175.4536 | 0.8476 | 4.42 | 760.3486 |
| 0.18026 | 137.0607 | 0.8223 | 4.45 | 760.3486 |
| 0.125188 | 95.18657 | 0.8213 | 4.47 | 760.3486 |
| 0.086925 | 66.09349 | 0.7819 | 4.49 | 760.3486 |
| 0.050239 | 38.19895 | 0.7246 | 4.52 | 760.3486 |

**Table A.3:** BET Analysis absorption values

| Relative Pressure | Volume Adsorbed ($cm^3/g$ STP) | 1/[VA*(Po/P)-1] |
|---|---|---|
| 0.069188 | 0.4548 | 0.163444 |
| 0.080233 | 0.4797 | 0.181832 |
| 0.100258 | 0.5194 | 0.214555 |
| 0.120282 | 0.5442 | 0.251248 |
| 0.140312 | 0.5626 | 0.290081 |
| 0.160328 | 0.5483 | 0.348235 |
| 0.199852 | 0.5522 | 0.452328 |
| 0.219762 | 0.5727 | 0.491775 |

the mass ratio of PVDF $x_1$ is calculated as follow:

$$x_1 = \frac{0.1}{0.94} = 0.1064 \tag{A.5}$$

So it's possible to find the solution's density assuming the volume of the total solution ($V_s$) equal to the volume of solvent (DMAc). With $m_1$ and $m_2$ are indicated respectively the mass of PVDF and DMAc and DMAc mass ratio is expressed as $x_2 = 1 - x_1$.

$$\frac{M_s}{V_s} = x_1 \frac{m_1}{V_s} + x_2 \frac{m_2}{V_s} = 0.1064 \cdot 0.1 + (1 - 0.1064) \cdot 0.94 = 0.85 \quad g/mL \tag{A.6}$$

**Table A.4:** BJH Adsorption Pore Distribution Report

| Pore Diameter ($\AA$) | Average Diameter ($\AA$) | Incremental Pore Volume | Cumulative Pore Volume ($cm^3$ |
|---|---|---|---|
| 1941.9 | 2291.2 | 0.019426 | 0.019426 |
| 934.7 | 1121.6 | 0.000476 | 0.019901 |
| 782.9 | 845.3 | 0.000912 | 0.020813 |
| 509.4 | 590.1 | 0.000688 | 0.021501 |
| 387.3 | 431.8 | 0.000708 | 0.022209 |
| 257 | 296.6 | 0.000767 | 0.022975 |
| 191.5 | 214.8 | 0.000524 | 0.0235 |
| 151.8 | 167.1 | 0.00031 | 0.02381 |
| 124.7 | 135.6 | 0.000246 | 0.024056 |
| 102.2 | 111.3 | 0.000268 | 0.024323 |
| 90.8 | 95.8 | 0.000099 | 0.024423 |
| 76.8 | 82.6 | 0.000113 | 0.024536 |
| 60.7 | 67 | 0.000064 | 0.024601 |

So from the solution density the mass amount of binder solution becomes: $Ms = \rho_s V_s = 0.85 \cdot 3.72 = 3.162 \quad g$

## A.4 Variable Resistance

The results obtained from the variable resistance test are shown below ( Tab. A.5, A.6, A.7) for the different conditions in the two cells.

**Table A.5:** Variable resistance test at different retention times and temperatures for the first cell fed with only raw waste water

| | $HRT$ = 1.8 h, T=21.5 °C | | | $HRT$ = 8.6 h, T=21.5 °C | | | $HRT$ = 8.6 h, T=37 °C | | |
|---|---|---|---|---|---|---|---|---|---|
| R($\Omega$) | V(V) | I(mA) | P($\mu$W) | V(V) | I(mA) | P($\mu$W) | V(V) | I(mA) | P($\mu$W) |
| 1110 | 0.275 | 0.25 | 68 | 0.237 | 0.21 | 51 | 0.211 | 0.19 | 40 |
| 1000 | 0.262 | 0.26 | 69 | 0.235 | 0.24 | 55 | 0.205 | 0.21 | 42 |
| 700 | 0.245 | 0.35 | 86 | 0.226 | 0.32 | 73 | 0.197 | 0.28 | 55 |
| 400 | 0.215 | 0.54 | 116 | 0.209 | 0.52 | 109 | 0.18 | 0.45 | 81 |
| 100 | 0.14 | 1.35 | 182 | 0.15 | 1.50 | 225 | 0.13 | 1.30 | 169 |
| 80 | 0.11 | 1.31 | 138 | 0.132 | 1.65 | 218 | 0.114 | 1.43 | 162 |
| 50 | 0.09 | 1.74 | 151 | 0.10 | 2.08 | 216 | 0.087 | 1.74 | 151 |
| 20 | 0.07 | 3.50 | 245 | 0.103 | 5.15 | 530 | 0.048 | 2.40 | 115 |

## A.5 Coulombic Efficiency

The Coulombic Efficiency for every sample taken from the cells at different retention times was calculated from equation (1.13) and the integral at the numerator was obtained from the data recorded by the Gamry potentiostat: the external resistance (100$\Omega$) was applied to the electrodes and other two clamps connected to the potentiostat collected the voltage across the cell which was afterwards divided by the resistance to get the current values. Total Coulombs produced by the cells are correspond to the integral of current over time so from Figures below a trapezoidal integral was accomplished using MATLAB function "trapz".

**Table A.6:** Variable resistance test at different retention times and temperatures for the first cell fed with solution amended with glucose

| | $HRT$ = 1.8 h, T=21.5 °C | | | $HRT$ = 8.6 h, T=21.5 °C | | | $HRT$ = 8.6 h, T=37 °C | | |
|---|---|---|---|---|---|---|---|---|---|
| R(Ω) | V(V) | I(mA) | P($\mu$W) | V(V) | I(mA) | P($\mu$W) | V(V) | I(mA) | P($\mu$W) |
| 1110 | 0.208 | 0.187 | 39 | 0.176 | 0.159 | 28 | 0.35 | 0.315 | 110 |
| 1000 | 0.198 | 0.198 | 39 | 0.172 | 0.172 | 30 | 0.224 | 0.224 | 50 |
| 700 | 0.188 | 0.269 | 50 | 0.163 | 0.233 | 38 | 0.214 | 0.306 | 65 |
| 400 | 0.17 | 0.425 | 72 | 0.147 | 0.368 | 54 | 0.192 | 0.480 | 92 |
| 100 | 0.115 | 1.150 | 132 | 0.097 | 0.970 | 94 | 0.126 | 1.260 | 159 |
| 80 | 0.102 | 1.275 | 130 | 0.082 | 1.025 | 84 | 0.109 | 1.363 | 149 |
| 50 | 0.076 | 1.520 | 116 | 0.062 | 1.240 | 77 | 0.08 | 1.600 | 128 |
| 20 | 0.041 | 2.050 | 84 | 0.032 | 1.600 | 51 | 0.041 | 2.050 | 84 |

**Table A.7:** Variable resistance test at different retention times and temperatures for the second cell fed with solution amended with glucose

| | $HRT$ = 1.8 h, T=21.5 °C | | | $HRT$ = 8.6 h, T=21.5 °C | | | $HRT$ = 8.6 h, T=37 °C | | |
|---|---|---|---|---|---|---|---|---|---|
| R(Ω) | V(V) | I(mA) | P($\mu$W) | V(V) | I(mA) | P($\mu$W) | V(V) | I(mA) | P($\mu$W) |
| 1110 | 0.25 | 0.225 | 56 | 0.272 | 0.245 | 67 | 0.342 | 0.308 | 105 |
| 1000 | 0.245 | 0.245 | 60 | 0.265 | 0.265 | 70 | 0.31 | 0.310 | 96 |
| 700 | 0.236 | 0.337 | 80 | 0.255 | 0.364 | 93 | 0.282 | 0.403 | 114 |
| 400 | 0.218 | 0.545 | 119 | 0.229 | 0.573 | 131 | 0.231 | 0.578 | 133 |
| 100 | 0.159 | 1.590 | 253 | 0.163 | 1.630 | 266 | 0.172 | 1.720 | 296 |
| 80 | 0.135 | 1.688 | 228 | 0.141 | 1.763 | 249 | 0.148 | 1.850 | 274 |
| 50 | 0.104 | 2.080 | 216 | 0.109 | 2.180 | 238 | 0.114 | 2.280 | 260 |
| 20 | 0.059 | 2.950 | 174 | 0.06 | 3.000 | 180 | 0.064 | 3.200 | 205 |